

t-SMILES 2: Hierarchical Structure Enhances the Generalizability of Linear Molecular Representation

Juan-Ni Wu, Tong Wang, Li-Juan Tang, Hai-Long Wu*, Ru-Qin Yu*

State Key Laboratory of Chemo/Biosensing and Chemometrics, College of Chemistry and Chemical Engineering, Hunan University, Changsha 410082, People's Republic of China

ABSTRACT

Encoding is the carrier of information. Artificial intelligence models possess basic capabilities in syntax, semantics, and reasoning, but these capabilities are sensitive to specific inputs. This study introduces TSIS (Simplified TSID) to the t-SMILES family, with the intention of conducting a more comprehensive and in-depth evaluation of t-SMILES. TSID has been demonstrated significantly outperforms classical SMILES, DeepSMILES, and SELFIES in previous research. Further analysis of this study reveals that the tree structure utilized by the t-SMILES framework is more effectively comprehensible than initially anticipated. Additionally, TSIS, along with their variants, demonstrate comparable performance to TSID and markedly surpass that of SMILES, SAFE, and SELFIES. Moreover, its format is more straightforward to read. Overall, the contrast analysis indicates that the hierarchical structure of t-SMILES enhances its generalizability. Concurrently, the evaluation of the generative models reveals that the GPT model exhibits the highest novelty-similarity scores. The VAE and diffusion models demonstrate robust capabilities in terms of interpolation, whereas the LSTM model encounters some challenges in parsing complex structures.

Introduction

Encoding acts as the carrier of information, ensuring that the intended message is accurately transmitted and understood. Effective representation of molecules is a crucial factor affecting the performance of artificial intelligence (AI) models. Unlike natural language processing (NLP) and image recognition, where deep learning has shown exceptional performance, one of the domain-specific challenges for AI assisted molecular discovery is the lack of a naturally applicable, complete and "raw" molecular representation[1].

Molecular descriptors are formal mathematical representations of a molecule, obtained by a well-specified algorithm, and applied to a defined molecular representation or a well-specified experimental procedure: the molecular descriptor is the final result of a logic and mathematical procedure which transforms chemical information encoded within a symbolic representation of a molecule into a useful number or the result of some standardized experiment[2]. Molecular descriptors serve as a foundational element in a wide range of chemistry-related scientific fields, including pharmaco-chemistry, environmental science, toxicology, ecotoxicology, health research, and quality control, among others. The scientific community's interest in molecular descriptors is evident from the vast array of over 5,000 descriptors proposed to date, originating from diverse theories and approaches documented in the literature. For those looking for a comprehensive review of molecular descriptors in the AI era, the following sources may be of interest:[3] [4] [5] [6]. These references provide an in-depth exploration of the development and application of molecular descriptors, particularly in the context of modern AI techniques.

Traditionally, molecules are represented as structure diagrams with bonds and atoms. However, molecules are also frequently represented as strings—linear sequences of alphanumeric symbols—known as Linear Molecular Representations (LMR). Each type of linear representation can be considered a chemical language, as these notations have a defined syntax, meaning not all possible combinations of characters will result in a 'chemically valid' molecule. Additionally, these notations have semantic properties, where the arrangement of elements within the string determines the corresponding molecule's physicochemical and biological properties. This characteristic allows deep learning methods developed for language and sequence modeling to be effectively applied to molecular strings, facilitating chemical language modeling[7]·[8]·[9].

Among LMRs, the Simplified Molecular Input Line Entry System (SMILES)[10] is a widely used choice for AI-driven molecular modeling tasks. However, due to the rule that parentheses and ring identifiers must be paired and the use of the Depth-First Search (DFS) algorithm to parse the molecular graph, SMILES code introduces long-range dependencies in grammar, posing challenges for state-of-the-art (SOTA) deep learning models. To address these issues, two alternative atom-based solutions, DeepSMILES (DSMILES)[11], and Self-referencing Embedded Strings (SELFIES)[12], were later proposed. However, both alternatives still struggle with complex grammar, making certain strings more difficult to parse[13]:[14]

Recently, two fragment-based solutions, t-SMILES[15] and SAFE[[16], have been introduced to address the limitations of SMILES. These two approaches use SMILES, instead of dictionary IDs, to describe molecular fragments, providing a more flexible and scalable method for molecular representation. In contrast, other ID-based solutions, like Group-SELFIES[17], encounter fundamental challenges such as in-vocabulary (IV) and out-of-vocabulary (OOV) issues, as well as the curse of dimensionality caused by high-dimensional sparse representations. These challenges limit the effectiveness and generalization capabilities of such ID-based methods.

SAFE sorts fragments by the number of atoms in descending order, which is compatible with classical SMILES through the use of an extended SMILES format known as CXSMILES, which was introduced by Chemaxon[18]. If the parameter "allowCXSMILES" is set to True, the SAFE string can be decoded directly using the RDKit[19] toolkit. In SAFE, the extracted fragments are sorted by size and concatenated, using a dot character (".") to mark new fragments in the representation, while preserving their corresponding attachment points.

t-SMILES is a tree-based linear molecular description framework that represents molecules using SMILES-type strings, which are generated by performing a breadth-first search (BFS) algorithm on a Full Binary Tree (FBT) formed from a fragmented molecular graph. In a previous study[15], three code algorithms—TSSA, TSDY, and TSID—were introduced. The key distinction between TSSA and TSDY/TSID lies in how they handle connecting points between fragments: in TSSA, two fragments share a real atom as the connecting point, while TSDY and TSID use a dummy atom (represented by the character "*" with or without an ID) to illustrate how the groups bond together. The t-SMILES algorithm follows a three-stage process:

1. **Generation of an Acyclic Molecular Tree (AMT):** The AMT is created to represent fragmented molecules.
2. **Transformation into a Full Binary Tree (FBT):** The AMT is converted into a FBT structure.
3. **Breadth-First Traversal:** Finally, a BFS of the FBT produces the t-SMILES string, which serves as the linear representation of the molecule.

This framework allows for a systematic and structured way of describing molecular structures, facilitating better analysis and interpretation in computational chemistry tasks.

In this study, we present a novel encoding algorithm for the t-SMILES family, named TSIS. TSIS directly generates strings by parsing the AMT using a BFS algorithm. This approach is feasible because dummy atoms with IDs (e.g., [n*]) can be utilized to construct a hierarchical logic that effectively represents the high-level molecular topological structure. In contrast to TSID, TSIS simplifies the process by eliminating the necessity for conversion from AMT to FBT, thereby streamlining the encoding procedure.

Language models (LMs) have essential capabilities in syntax, semantics, and reasoning. A key goal of using NLP models for molecular modeling is to enable AI models to reason about the information hidden in molecular descriptors. Transformers[20] are considered the leading models in recent NLP research and will be the primary model used in this study to assess syntax and semantics. Additionally, LSTM models will also be evaluated for their performance in syntax and semantics analysis for comparative purposes.

By definition, a Transformer is invariant with respect to reordering of the input. However, language is inherently sequential and word order is essential to the semantics and syntax of an utterance[21][22]. Recent studies have shown that language models pretrained and/or fine-tuned on randomly permuted sentences exhibit competitive performance on GLUE[23], putting into question the importance of word order information. Somewhat counter-intuitively, some of these studies also report that position embeddings appear to be crucial for models’ good performance with shuffled text[24].

To thoroughly investigate the impact of the fragment order on the Fragment-Based Linear Molecular Representation (FLMR) system, we introduce three additional encoding algorithms derived from TSIS: TSISD, TSISO, and TSISR. TSISD utilizes a depth-first search (DFS) algorithm on the AMT, TSISO sorts fragments by length, and TSISR randomly shuffles the

fragments. These variations allow us to explore how different ordering methods affect the performance and efficacy of the FLMR system.

In a previous study[15], the distribution of tokens and nesting depth were examined. In this study, we initiate experiments by analyzing syntax and semantics on the ChEMBL dataset, employing Transformer and LSTM[25] models across various code algorithms.

Experiments reveal that, somewhat counterintuitively, the tree structure used by TSID is learned more easily than expected, regardless of whether Transformer or LSTM models are used. This may be due to the assertion that layered architectures can reduce the sample complexity of a non-trivial learning problem [26]. Additionally, the order information in TSISO and SAFE is also learned relatively easily, and TSISO appearing to be more straightforward to learn than SAFE, likely due to its reduced long-term dependency on syntax. In terms of semantics, SMILES, TSID, TSIS, and SAFE exhibit comparable performance. However, the SELFIES model tends to produce a greater number of molecules with fewer atomic rings.

In addition to autoregressive models, two latent variable models—VAE[27][28] and the diffusion model[29]—are evaluated on ChEMBL as part of a comprehensive assessment. System experiments across ChEMBL, Zinc, and other complex molecules demonstrate that both TSID and TSIS achieve a high level of fit with the training data, comparable to SMILES in terms of physicochemical properties, with t-SMILES achieving higher novelty scores. Furthermore, TSID and all sub-algorithms of TSIS outperform SELFIES and SAFE in distribution learning metrics.

Algorithms

TSIS represents a novel extension to the t-SMILES family while maintaining the core principles of the t-SMILES framework. The primary distinction between TSIS and TSID is that TSIS generates strings by parsing the AMT rather than the FBT using a BFS algorithm. The construction of a TSIS string from a molecule involves two key steps: first, the molecule is fragmented using a selected fragmentation algorithm to create the AMT; second, the AMT is traversed using the BFS algorithm to produce the TSIS sequence. To reconstruct a molecule from a TSIS string, follow these two steps:

1. **Decompose the TSIS String:** Reconstruct the Acyclic Molecular Tree (AMT) from the TSIS string.

2. **Assemble Molecular Fragments:** Use the selected algorithm to piece together the molecular fragments, generate the molecular graph, and then optimize it to produce the final molecule.

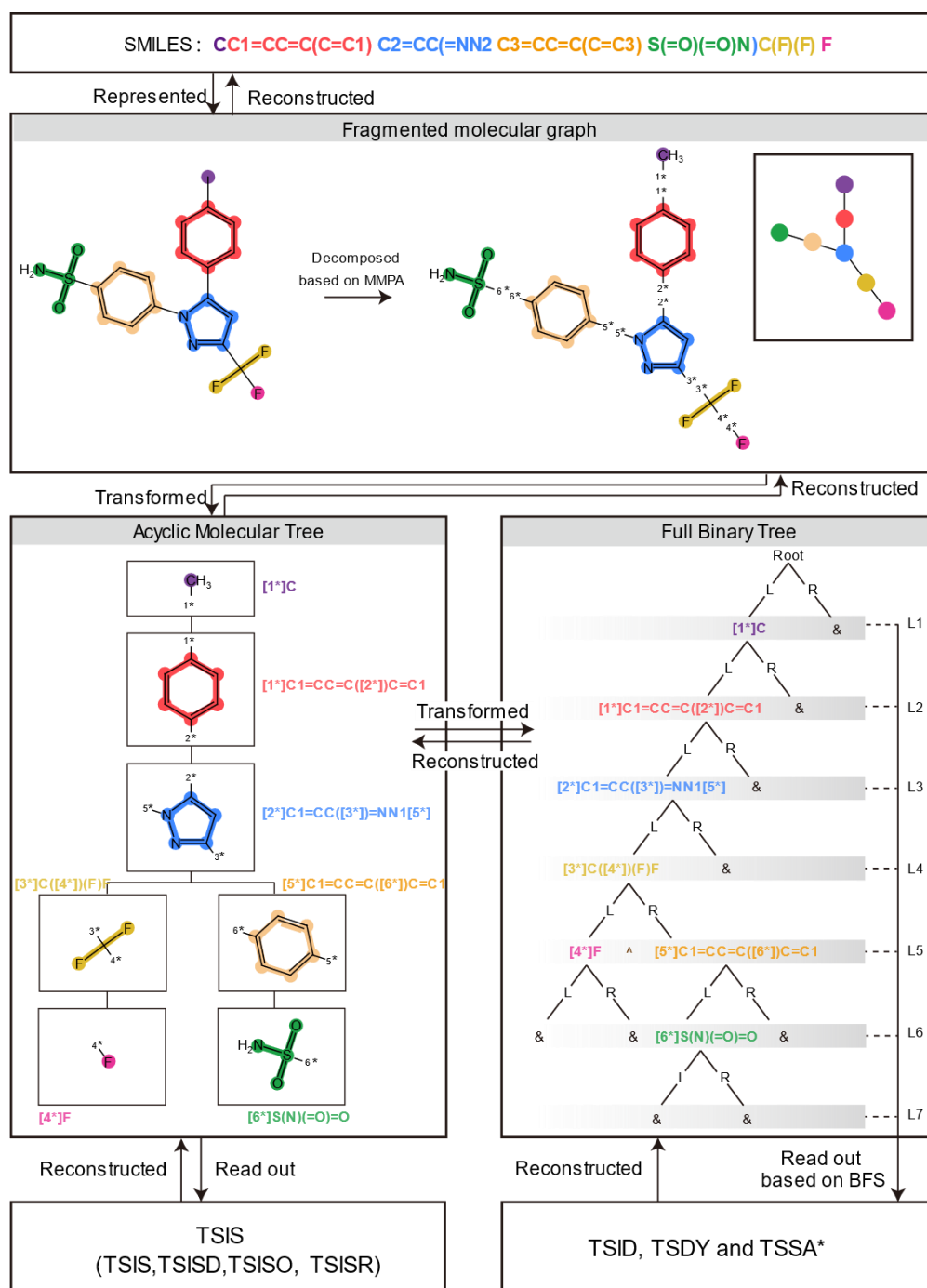


Fig.1 Overview of the t-SMILES algorithm. In a prior study[15], TSID, TSDY, and TSSA were introduced, deriving from FBT. TSIS and its variants TSISD, TSISO, and TSISR come from AMT. TSIS, TSID, TSDY and TSSA use BFS algorithm to parse AMT or FBT. TSISD use DFS to parse AMT. TSISO sort fragment in order. TSISR shuffles fragments randomly. It should be noted that the logic used to link fragments of TSSA differs from that used for TSDY, TSID, and TSIS.

Table 1 provides a summary of the different t-SMILES codes based on the MMPA fragmentation algorithm applied to the molecule Celecoxib.

Table 1. Codes of TSID and TSIS. TSIS: Breadth-first search algorithm on AMT. TSISD: Depth-first search algorithm on AMT. TSISO: Sorted TSIS based on length of fragments. TSISR: Randomly shuffle fragments of TSIS, the code maybe different based on different random seed.

Code Algorithm	Celecoxib	Length
TSID_M (BFS)	[1*]C&[1*]C1=CC=C([2*])C=C1&[2*]C1=CC([3*])=NN1[5*]&[3*]C([4*])(F)F&[4*]F^[5*]C1=CC=C([6*])C=C1&&[6*]S(N)(=O)=O&&&	114
TSIS_M (BFS)	[1*]C^[1*]C1=CC=C([2*])C=C1^[2*]C1=CC([3*])=NN1[5*]^^[3*]C([4*])(F)F^[5*]C1=CC=C([6*])C=C1^[4*]F^[6*]S(N)(=O)=O	110
TSISD_M (DFS)	[1*]C^[1*]C1=CC=C([2*])C=C1^[2*]C1=CC([3*])=NN1[5*]^^[3*]C([4*])(F)F^[4*]F^[5*]C1=CC=C([6*])C=C1^[6*]S(N)(=O)=O	110
TSISO_M (Order)	[2*]C1=CC([3*])=NN1[5*]^^[1*]C1=CC=C([2*])C=C1^[5*]C1=CC=C([6*])C=C1^[3*]C([4*])(F)F^[6*]S(N)(=O)=O^[1*]C^[4*]F	110
TSISR_M (Random)	[6*]S(N)(=O)=O^[1*]C^[2*]C1=CC([3*])=NN1[5*]^^[1*]C1=CC=C([2*])C=C1^[3*]C([4*])(F)F^[5*]C1=CC=C([6*])C=C1^[4*]F	110

Results

To evaluate the performance of different LMRs, experiments will be conducted on ChEMBL, Zinc, and complex molecules using various chemical language models (CLMs), including LSTM, Transformer, VAE, and diffusion models. Initially, syntax and semantics will be analyzed using Transformer and LSTM models. Following this, a comprehensive evaluation will be performed using all four CLMs for distribution learning tasks.

Syntax and semantics

The true challenge for CLMs lies not in mastering the numerous elementary atom-bonding rules, but in understanding the complex rules that persist even after the basics are acquired [30]. In NLP, syntax and semantics are two fundamental concepts that focus on different aspects of language. **Syntax** refers to the set of rules, principles, and processes that govern the structure of sentences in a language. It concerns how words combine to form phrases, clauses, and sentences, determining the correct word order and hierarchical structure within sentences. **Semantics** deals with the meaning of words, phrases, sentences, and texts. It focuses on how language conveys meaning and how that meaning is interpreted by speakers and listeners.

In SMILES, a syntactic specification [31] outlines how atoms, bonds, parentheses, digits, and other symbols are represented, while a semantic specification describes how these symbols are interpreted to form a valid molecule. For example, the syntax defines how ring closures are written, but the semantics ensures that these closures are correctly paired. Similarly, while the syntax dictates the representation of atomic elements, the semantics determines whether a ring system is aromatic.

SMILES offers a simplified definition of aromaticity, which can be represented in two ways: **Kekulé Form**: Uses alternating single and double bonds with uppercase symbols for atoms. For example, the Kekulé form of the molecule Indane is ‘C1=CC=CC(CCC2)=C12’.

Aromatic Symbols: Uses lowercase letters for aromatic atoms, such as 'c' for aromatic carbon, with no need for bond symbols. For example, the SMILES representation of Indane is 'c1ccc2CCCCc2c1'. Although the Kekulé form obscures the inherent uniformity of bonds in aromatic rings from a chemical perspective[31], it provides a more formatted representation by explicitly detailing partial bond information.

Syntax

From a syntactic perspective, t-SMILES uses a tree-based data structure to represent high-level molecular topology. For instance, the skeleton of TSID_M for the molecule Celecoxib can be represented as: 'A&A&A&A^A&&A&&&'. This approach may initially seem more complex than SMILES. Additionally, in TSID and TSIS, dummy atoms with IDs (e.g., [n*]) are used to denote joint points, which should appear in pairs across sub-fragments. Moreover, the hidden pattern in TSISO and SAFE involves the order of fragments.

To reveal the impact of syntactic information, such as tree structure and fragment order, experiments were conducted on ChEMBL and a subset of 100,000 molecules using both Transformer and LSTM models. The results of these experiments are summarized in Table 2 and Table 3.

Overall, it is somewhat surprising that the FBT structure used by TSID is relatively straightforward to learn, even more so than the order used by TSISO. Analogous to natural language, the symbol "&^" in LMRs can be viewed as a marker character for constructing syntax. This finding aligns with research in NLP, which suggests that syntactic abilities are acquired with remarkable consistency and reliability early in the pre-training process[32]. Specifically, syntactic rules are often learned within the first 20% of masked language model pre-training, as demonstrated by various syntactic generalization suites[33][34].

Tables 2 illustrate that when the GPT model was trained with 10 rounds on 10,000 training molecules, the FBT was accurately learned and generated with a score of 0.987, indicating a high degree of accuracy. Upon reaching approximately 154,000 training data points, only three generated strings were incorrectly parsed as correct FBT.

A comparison of the SAFE and TSISO, both of them sort fragemments in order, reveals that TSISO is more efficient at learning syntax information than SAFE.

Table.2 Results for the Distribution-Learning Benchmarks on **ChEMBL**(about 1,540,000 molecules) and a subset of 100,000 molecules using **GPT**. Levenshtein distance (LVSD) is calculated to evaluate distance.

Model	Valid	Unique	Novelty	KLD	FCD	LVSD=0 Or Correct FBT	LVSD=2	nFrag=1
SMILES[R10] (10*100K)	0.925	0.923	0.904	0.978	0.840	-	-	-
SMILES[R1] (1*1540k)	0.947	0.947	0.924	0.979	0.874	-	-	-
SMILES[R10] (10*1540k)	0.980	0.979	0.907	0.992	0.906	-	-	-
Kekule[R10] (10*100K)	0.962	0.962	0.943	0.974	0.855	-	-	-
Kekule[R1] (1*1540k)	0.969	0.968	0.947	0.976	0.859	-	-	-
Kekule[R10] (10*1540k)	0.986	0.984	0.916	0.993	0.908	-	-	-
SELFIES[R10] (10*100K)	1.000	1.000	0.988	0.921	0.509	-	-	-
SELFIES[R1] (1*1540k)	1.000	1.000	0.987	0.942	0.634	-	-	-
SELFIES[R10] (10*1540k)	1.000	1.000	0.958	0.979	0.857	-	-	-
SAFE[R10] (10*100K)	0.640	0.620	0.608	0.943	0.697	0.611	0.906	0.629
SAFE[R1] (1*1540k)	0.706	0.689	0.675	0.958	0.736	0.620	0.900	0.694
SAFE[R10] (10*1540k)	0.845	0.839	0.809	0.974	0.852	0.658	0.940	0.846
TSISO_B[R10] (10*100K)	1.000	0.996	0.960	0.964	0.797	0.912	0.993	-
TSISO_B[R1] (1*1540k)	1.000	0.997	0.963	0.966	0.834	0.910	0.992	-
TSISO_B[R10] (10*1540k)	1.000	0.999	0.932	0.988	0.902	0.936	0.999	-
TSID_B[R10] (10*100K)	0.999	0.998	0.972	0.971	0.832	0.987 (128 wrong in 10k)	-	-
TSID_B[R1] (1*1540k)	1.000	0.999	0.969	0.978	0.863	1.000 (3 wrong in 10k)	-	-
TSID_B[R10] (10*1540k)	1.000	0.999	0.941	0.989	0.909	1.000 (4 wrong in 10k)	-	-

Table.3 Results for the Distribution-Learning Benchmarks on **ChEMBL**(about 1,540,000 molecules) and a subset of 100,000 molecules using **LSTM**. Levenshtein distance (LVSD) is calculated to evaluate distance.

Model	Valid	Unique	Novel	KLD	FCD	LVSD=0 Or Correct FBT	LVSD=2	nFrag=1
SMILES[R10] (10*100K)	0.812	0.811	0.792	0.957	0.753	-	-	-
SMILES[R1] (1*1540k)	0.888	0.888	0.868	0.938	0.741	-	-	-
SMILES[R10] (10*1540k)	0.956	0.955	0.914	0.930	0.806	-	-	-
Kekule[R10] (10*100K)	0.917	0.916	0.904	0.961	0.733	-	-	-
Kekule[R1] (1*1540k)	0.961	0.961	0.939	0.917	0.729	-	-	-
Kekule[R10] (10*1540k)	0.979	0.979	0.939	0.933	0.816	-	-	-
SELFIES[R10] (10*100K)	1.000	1.000	0.991	0.907	0.335	-	-	-
SELFIES[R1] (1*1540k)	1.000	1.000	0.991	0.854	0.417	-	-	-
SELFIES[R10] (10*1540k)	1.000	1.000	0.979	0.901	0.707	-	-	-
SAFE[R10] (10*100K)	0.501	0.456	0.450	0.902	0.466	0.618	0.914	0.461
SAFE[R1] (1*1540k)	0.605	0.581	0.572	0.895	0.593	0.660	0.937	0.590
SAFE[R10] (10*1540k)	0.736	0.725	0.704	0.921	0.741	0.658	0.940	0.729
TSISO_B[R10] (10*100K)	1.000	0.991	0.941	0.905	0.579	0.910	0.992	-
TSISO_B[R1] (1*1540k)	1.000	0.992	0.949	0.908	0.668	0.901	0.995	-
TSISO_B[R10] (10*1540k)	1.000	0.998	0.947	0.925	0.777	0.945	0.999	-
TSID_B[R10] (10*100K)	1.000	0.995	0.957	0.963	0.715	0.997 (29 wrong in 10k)	-	-
TSID_B[R1] (1*1540k)	1.000	0.998	0.963	0.935	0.709	1.000 (1 wrong in 10k)	-	-
TSID_B[R10] (10*1540k)	1.000	0.999	0.963	0.950	0.795	1.000 (0 wrong in 10k)	-	-

With regard to the SAFE algorithm, the valid scores are significantly less than those for SMILES, indicating that SAFE is a more challenging code to parse than SMILES. This may be interpreted as corroborating the analysis presented in the discussion section, which posits that SAFE does not diminish long-term dependence but, instead, may potentially exacerbate it.

Furthermore, it can be observed that when LVSD is set to zero, the resulting lower score indicates that a significant proportion of the generated data is not in the expected order. Furthermore, nFrag (number of fragments in generated string) is calculated. A value of nFrag greater than one indicates that the SAFE model generates some fragmented sets that cannot be parsed as a whole molecule. The lower score of LVSD and nFrag indicates that the SAFE code is more complex to learn than TSISO.

The SMILES and Kekule-style approaches differ in their descriptions. In general, the Kekule-style approach yields higher score on validity and other four metrics. This indicates that the Kekule-style approach may be more efficient than the classical SMILES approach to describe molecules.

A comparison of the results from LSTM and Transformer models reveals that both are capable of efficiently identifying the hidden hierarchical patterns in trees or orders. Notably, LSTM models achieve slightly higher scores than GPT models in learning this specific type of syntax. However, a deeper analysis shows that the LSTM model generates fewer and shorter novel FBTs, as illustrated in SI.Fig.E.3. This discrepancy might contribute to the observed high scores.

A comprehensive evaluation of the capabilities of LSTM and Transformer models is essential for advancing the design of subsequent neural networks. This finding provides valuable insights into the ability of LSTM and Transformer models to parse hierarchical information in NLP[35][36][37][38][39], though it remains an open area for further research.

Semantics

Semantic analysis—the study of the meaning of words, phrases, sentences, and texts—is a fundamental aspect of language comprehension. A deep understanding of semantics is essential for reasoning, as it enables the interpretation of context, relationships, and implications within language. For AI models, mastering semantics is crucial because it reflects their ability to grasp and manipulate meaning, which is a key indicator of progress toward human-like intelligence.

In this study, the metric N_AromaticRings (the number of aromatic rings for a molecule), as illustrated in Fig.2 and Fig.3, is calculated to evaluate the performance of AI models in handling aromaticity, which is the key semantic concept in LMRs.

With the exception of SELFIES, the remaining five LMRs employ "SMILES" as the fundamental description, demonstrating comparable performance in learning and generating

atomic rings.

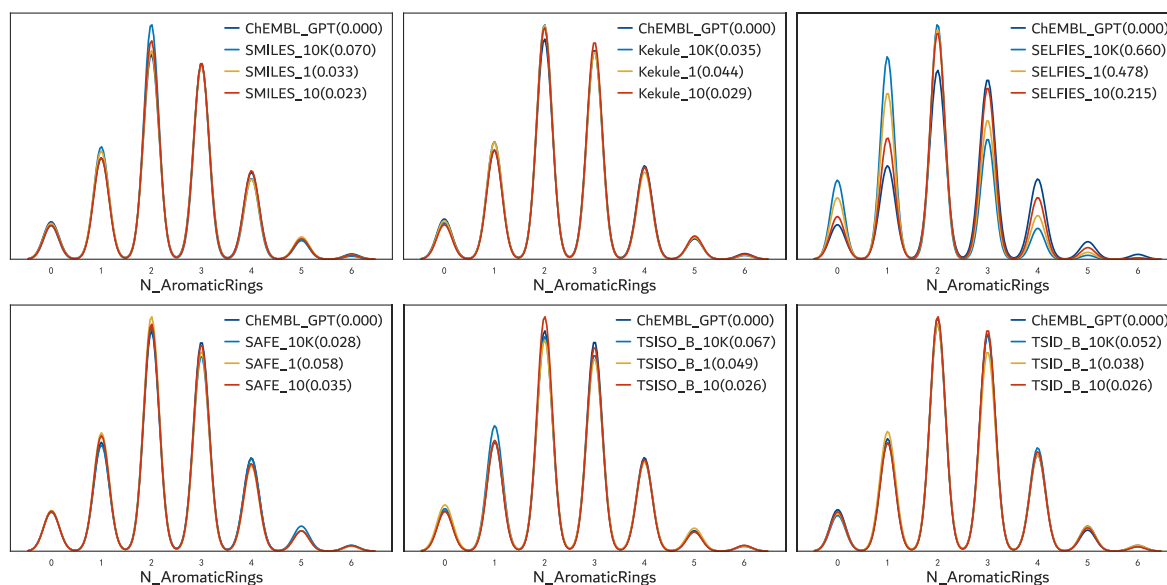


Fig.2 The number of aromatic rings for a molecule (N-AromaticRings) on ChEMBL using GPT.

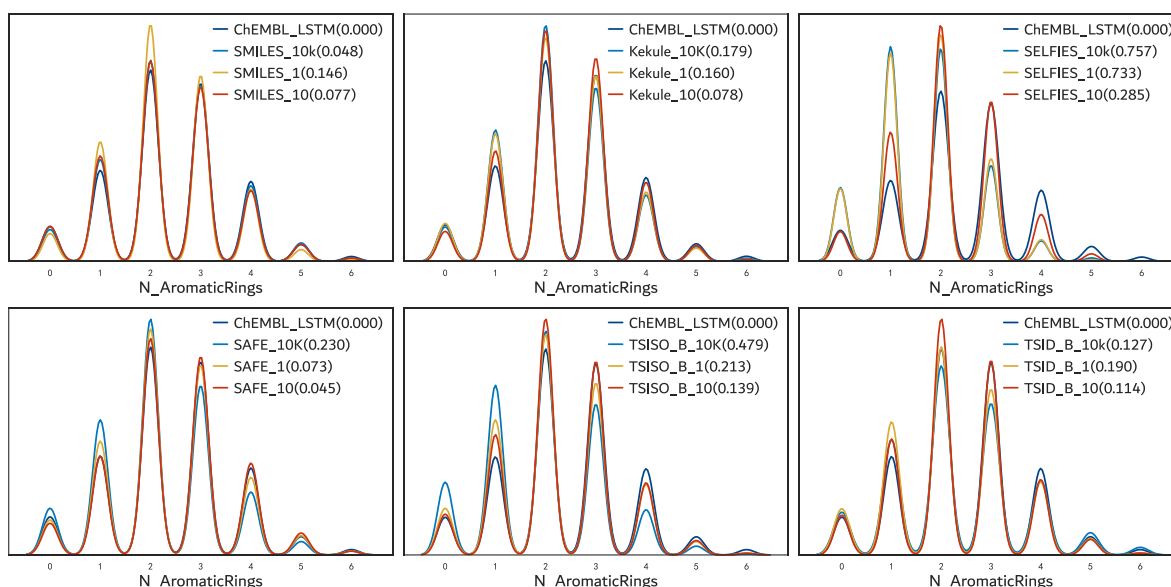


Fig.3 The number of aromatic rings for a molecule (N-AromaticRings) on ChEMBL using LSTM.

The SMILES and Kekule-style approaches differ in their aromaticity descriptions. Both methods are relatively straightforward to learn and generate atomic rings, although the SMILES without the Kekule-style approach may require slightly more effort at the beginning. However, at the final stage, they achieve almost the same relative high performance.

In terms of SELFIES, which generates more molecules with fewer atomic rings, as illustrated in panel c, where larger values are observed on 0, 1, and 2 and smaller values on 4, 5, and 6, this is consistent with the statement that the approach of SELFIES focus on robustness making some SELFIES strings more challenging to read[14].

A comparison of GPT and LSTM models reveals that GPT models demonstrate superior performance in the learning of semantic information. In general, all LSTM-based models achieve lower N-AromaticRings scores than GPT-based models, as demonstrated in Fig.3.

LSTM Models on ChEMBL

In examining the performance of LSTM models, we observed some findings that differed from those observed in GPT, VAE, and diffusion models. To confirm these findings and conduct a comprehensive analysis, we conducted additional experiments. In total, three types of model were trained. The first model is of a larger scale and has a hidden size of 1024 (MH1024), while the other two models have a hidden size of 512 (MH512). One of the MH512 models uses single characters as tokens, whereas the other utilizes multiple characters, such as '[CH2]', as tokens. The results are presented in Table 4 and Fig.4.

In comparison to the baseline model, which was published in GuacaMol[43], the MH1024 model employs a smaller batch size of 128, resulting in slightly lower novelty and FCD scores. Conversely, the MH512 model, which was utilized as the base model for the goal-direction task in a previous study[15], exhibits a lower FCD score but a higher novelty score.

Table.4 Results for the Distribution-Learning Benchmarks on ChEMBL using LSTM. R10 in [R*-3-*-b*] means training 10 epochs. 3 means the layer is 3. 512 and 768 means the hidden size is 512 or 1024. Bs512 or bs128 means batch size is 512 or 128. [mpl] means the multiple characters are used as tokens, [char] means the single character is used as token.

Model	Valid	Unique	Novelty	KLD	FCD
LSTM_SMILES[R20_3_1024_bs512][25],[43]	0.959	1.000	0.912	0.991	0.913
LSTM_SMILES[R10-3-1024-b128][mpl]	0.961	0.961	0.902	0.941	0.844
LSTM_SMILES[R10-3-512-b128][char][15]	0.954	0.954	0.919	0.975	0.866
LSTM_SMILES[R10-3-512-bs128][mpl]	0.956	0.955	0.914	0.930	0.806
LSTM_SELFIES[R10-3-1024-b128][mpl]	1.000	1.000	0.956	0.917	0.773
LSTM_SAFE[R10-3-1024-b128][mpl]	0.777	0.768	0.739	0.929	0.761
LSTM_TSDY_B[R10-3-1024-b128][mpl]	1.000	0.999	0.944	0.924	0.817
LSTM_TSID_B[R10-3-1024-b128][mpl]	1.000	0.999	0.936	0.952	0.829
LSTM_TSID_B[R10-3-1024-b128][mpl]	1.000	0.999	0.940	0.945	0.841
LSTM_TSISO_B[R10-3-1024-b128][mpl]	1.000	0.996	0.936	0.926	0.821
LSTM_TSISR_B[R10-3-1024-b128][mpl]	1.000	0.997	0.951	0.943	0.815
LSTM_TSID_S[R10-3-1024-b128][mpl]	1.000	0.999	0.942	0.943	0.808
LSTM_TSIS_S[R10-3-1024-b128][mpl]	1.000	0.995	0.943	0.947	0.815
LSTM_TSSA_M[R10-3-512-bs128][mpl]	1.000	0.999	0.966	0.963	0.782
LSTM_TSDY_M[R10-3-512-bs128][mpl]	1.000	1.000	0.981	0.902	0.754
LSTM_TSID_M[R10-3-512-bs128][mpl]	1.000	0.999	0.968	0.925	0.783
LSTM_TSIS_M[R10-3-512-bs128][mpl]	1.000	0.996	0.959	0.931	0.794
LSTM_TSISO_M[R10-3-512-bs128][mpl]	1.000	0.996	0.959	0.931	0.794
LSTM_TSISR_M[R10-3-512-bs128][mpl]	1.000	0.996	0.976	0.924	0.693
LSTM_TSSA_S[R10-3-512-bs128][mpl]	1.000	0.995	0.980	0.950	0.690
LSTM_TSDY_S[R10-3-512-bs128][mpl]	1.000	0.999	0.968	0.945	0.796
LSTM_TSID_S[R10-3-512-bs128][mpl]	1.000	1.000	0.964	0.936	0.799
LSTM_TSIS_S[R10-3-512-bs128][mpl]	1.000	0.996	0.961	0.948	0.824
LSTM_TSISO_S[R10-3-512-bs128][mpl]	1.000	0.995	0.962	0.953	0.826
LSTM_TSISR_S[R10-3-512-bs128][mpl]	1.000	0.996	0.969	0.938	0.796

A comparative analysis of the tested LSTM and GPT models reveals that, on average, the

FCD scores of LSTM models are generally lower than those of GPT models. This finding corroborates the observation made in the syntax and semantics section that LSTM models generate a smaller number of and shorter novel FBTs. It is also noteworthy that TSID exhibits slightly lower FCD scores than TSIS in general, which is in contrast with the performance of GPT. It can therefore be reasonably concluded that GPT models leverage the self-attention mechanism, which allows them to attend to all tokens in the sequence simultaneously, thereby enabling a comprehensive understanding of global structure. In contrast, the experimental results demonstrate that LSTM models face challenges in processing long-range dependencies and complex structures, although LSTM is able to parse the pattern of t-MSILES correctly.

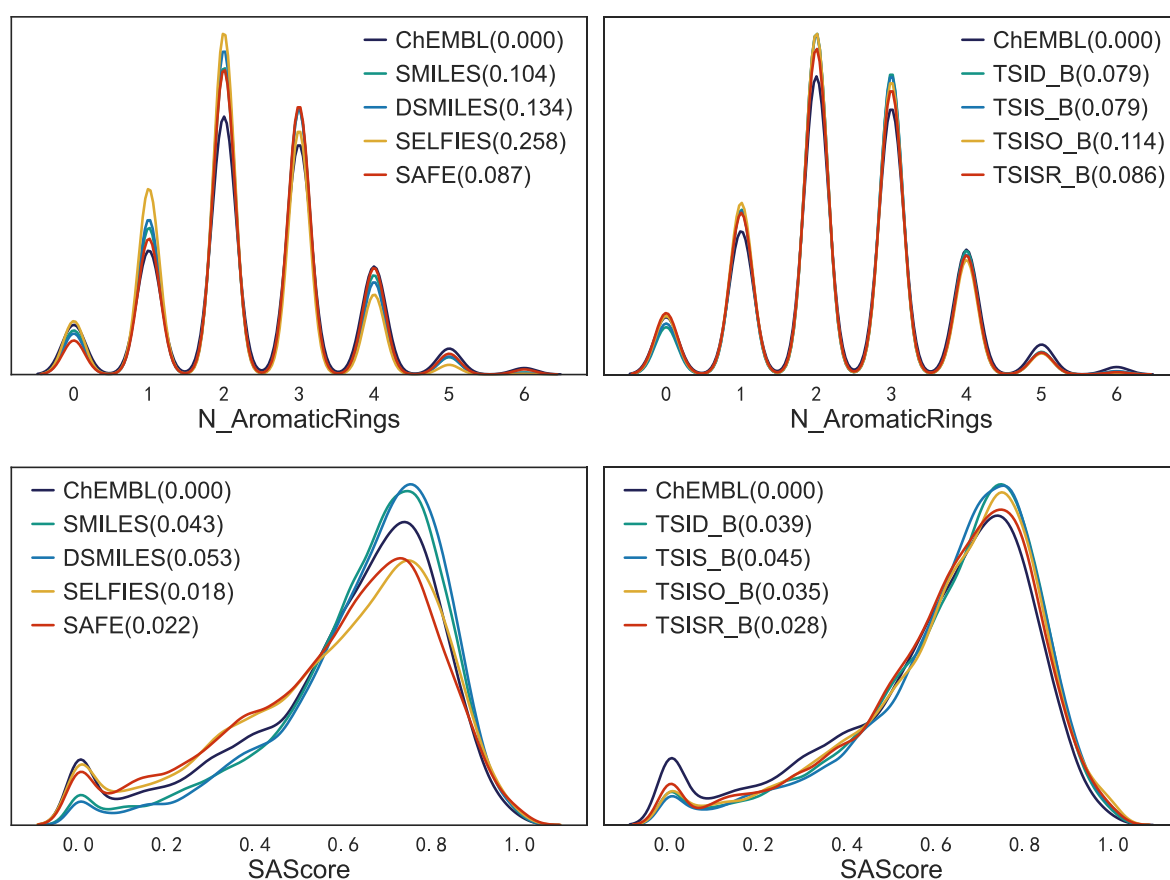


Fig.4 Physicochemical Properties on **ChEMBL** using **LSTM**. Models based on SELFIE tend to yield a greater number of molecules with a lower number of aromatic rings. In comparison to the SELFIES and SAFE models, the models based on t-SMILES and SMILES demonstrate a better fit to the training dataset.

In consideration of the various LMRS, with the exception of TSSA, the t-SMILS models demonstrate superior performance on both novelty and FCD scores when compared to SAFE. When evaluated against SELFIES, the t-SMILES models exhibit higher FCD scores when the model architecture is similar. This indicates that the t-SMILES code is more easily comprehensible than SELFIES and SAFE.

In comparison to SMILES and SELFIES, numerous t-SMILES models exhibit high novelty scores when the FCD is similar.

In examining the t-SMILES family, it can be observed that TSISR exhibits a lower FCD score in comparison to TSID and TSIS, a result that is analogous to the performance observed in GPT, VAE models.

The figures of physicochemical properties indicate that TSID and TSIS exhibit higher performance than other alternatives.

GPT Models on ChEMBL

This experiment is designed to conduct a comprehensive and systematic evaluation of the performance of different LMRs using a Transformer architectural approach. So, BRICS, MMPA, and Scaffold are used as fragmentation algorithm to get t-SMILES codes. Additionally, the SMILES, SELFIES, and SAFE algorithms will serve as a baseline for comparison. Given the complexity of SAFE, a larger model([R15-768]: hidden size if 768, training round is 15) is trained to generate more valid molecules. The results are presented in Table 5 and Fig.5.

Table.5 Results for the Distribution-Learning Benchmarks on **ChEMBL** using **GPT**. R10 means training 10 epochs. 256 or 768 in[R*-*] means the hidden size of model.

Model	Valid	Unique	Novelty	KLD	FCD	LVSD=0 Or Wrong FBT	LVSD=2
MoIGPT[40]	0.981	0.998	1.000	0.992	0.907		
SMILES[R10-256][15]	0.980	0.979	0.907	0.992	0.906	-	-
DSMILES[R15-256][15]	0.910	0.908	0.845	0.992	0.896	-	-
SELFIES[R10-256][15]	1.000	1.000	0.958	0.979	0.857		-
SAFE[R10-256]	0.845	0.839	0.809	0.974	0.852	0.645	0.929
SAFE[R15-768]	0.911	0.906	0.746	0.992	0.896	0.661	0.934
TSSA_B_[R20][15]	1.000	0.995	0.956	0.972	0.708	-	-
TSDY_B_[R15][15]	1.000	0.999	0.960	0.977	0.854	-	-
TSID_B[R10-256][15]	1.000	0.999	0.941	0.989	0.909	-	-
TSIS_B[R10-256]	1.000	0.990	0.932	0.990	0.902	-	-
TSISO_B[R10-256]	1.000	0.999	0.932	0.988	0.902	0.946	0.996
TSISR_B[R10-256]	1.000	0.999	0.952	0.979	0.881	-	-
TSSA_M_[R50][15]	1.000	0.996	0.970	0.982	0.808	-	-
TSDY_M_[R15][15]	1.000	0.998	0.970	0.960	0.852	-	-
TSID_M[R10-256][15]	0.999	0.998	0.942	0.968	0.892	-	-
TSIS_M[R10-256]	1.000	0.998	0.936	0.990	0.907	-	-
TSISO_M[R10-256]	1.000	0.998	0.938	0.991	0.907	0.938	0.995
TSISR_M[R10-256]	1.000	0.996	0.970	0.969	0.842	-	-
TSISD_M[R10-256]	1.000	0.998	0.935	0.991	0.904	-	-
TSSA_S_[R50][15]	1.000	0.998	0.977	0.966	0.795	-	-
TSDY_S_[R15][15]	1.000	0.999	0.955	0.982	0.878	-	-
TSID_S[R10-256][15]	1.000	0.999	0.933	0.991	0.909	-	-
TSIS_S[R10-256]	1.000	0.997	0.930	0.991	0.906	-	-
TSISO_S[R10-256]	1.000	0.997	0.940	0.991	0.907	0.985	1.000
TSISR_S[R10-256]	1.000	0.998	0.955	0.984	0.891	-	-

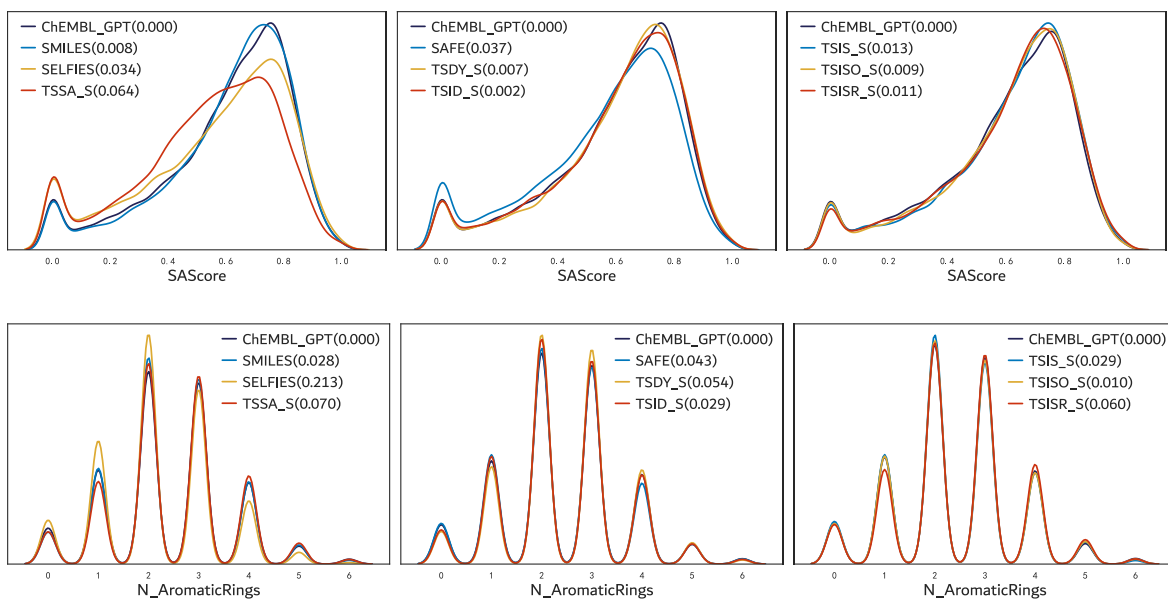


Fig.5 Physicochemical Properties on **ChEMBL** using **GPT**. Models based on SELFIE tend to yield a greater number of molecules with a lower number of aromatic rings. In comparison to the SELFIES and SAFE models, the models based on t-SMILES demonstrate a superior fit to the training dataset, with the exception of TSSA, which exhibits a similarity to SMILES-based models. This superiority is observed regardless of the order of the fragments in TSIS and TSISO.

Table 5 indicates that the model SAFE[R10-256] scores the lowest across all tested models, indicating that the SAFE string is more challenging to parse compared to other LMRs. This supports the findings from the Syntax section, where the logic of SAFE made the analysis of paired numbers and syntax more difficult. Additionally, the results reveal that a larger model, SAFE[R15-768], which generates more valid molecules, achieves a higher FCD score but a lower novelty score.

A comparison between SAFE and TSISO-based models reveals that TSISO-based models significantly outperform SAFE-based models across all calculated metrics. Additionally, the analysis of physicochemical properties shown in Fig. 4 indicates that SAFE models receive the lowest scores compared to TSID, TSIS, and SMILES.

The analysis of t-SMILES code algorithms, including TSID, TSIS, TSISD, TSIO, and TSISR, shows that these algorithms exhibit comparable performance and significantly outperform SMILES, SELFIES, and SAFE. Despite differences in the order of sub-fragments among TSIS, TSISD, TSIO, and TSISR, the CLMs trained on these algorithms achieve relatively better scores. For a detailed comparative analysis, please refer to the discussion section.

In conclusion, the experiment on ChEMBL indicates that Transformer models trained on TSIS typically generated novel molecules at a higher rate than models trained on SMILE and

SAFE. Furthermore, models trained on TSISO demonstrated superior performance in terms of FCD scores compared with SELFIES and SAFE. The TSIS code algorithm is flexible to sort fragment-like TSISO for different purposes, and all of them achieve similar performance with TSID. In terms of physicochemical properties, TSIS and TSID demonstrated superior performance in fitting the training data compared to SAFE and SELFIES.

VAE Models on ChEMBL

As the classical latent variable model, the development of variational autoencoder (VAE) models can be traced back to denoising autoencoders, which were introduced by P. Vincent and colleagues[27]. The true generative VAEs were introduced by D. P. Kingma and colleagues[28]. In a pioneering work[41], VAE was employed for molecule generation, thereby inaugurating a novel strategy in de novo drug design. In this section, the VAE model, which was published in MOSES[42], is utilized to assess t-SMILES codes and other LMPs, as illustrated in Table 6 and Fig. 6.

Table.6 Results for the Distribution-Learning Benchmarks on ChEMBL using VAE. All models are trained on GPU: NVIDIA Tesla NVIDIA V100s. Two models, with hidden sizes of 768 and 512, were trained. A potential explanation for the observed differences in outcomes is that the larger VAE model, designated as (3-z256-dh768-qh768-bs256-d0.5), may not have undergone sufficient training yet.

Model	Valid	Uniq	Novel	KLD	FCD
CharacterVAE[41][43] (3-z128-dh512-qh256-bs512-d0.5)	0.870	0.999	0.974	0.982	0.863
VAE_SMILES[768][mpl][768]	0.886	0.885	0.857	0.971	0.827
VAE_DSMILES[768]	0.828	0.821	0.757	0.969	0.835
VAE_SELFIES[768]	1.000	1.000	0.951	0.957	0.703
VAE_SAFE[768]	0.682	0.662	0.625	0.960	0.741
VAE[gru]_TSSA_B[768][mpl]	1.000	0.959	0.922	0.959	0.623
VAE[gru]_TSDY_B[768][mpl]	1.000	1.000	0.953	0.969	0.820
VAE[gru]_TSID_B[768][mpl]	1.000	0.999	0.904	0.984	0.878
VAE[gru]_TSIS_B[768][mpl]	1.000	0.994	0.934	0.973	0.843
VAE[gru]_TSISO_B[768][mpl]	1.000	0.995	0.913	0.973	0.848
VAE[gru]_TSISR_B[768][mpl]	1.000	0.994	0.934	0.967	0.819
VAE[gru]_TSID_M[768][mpl]	1.000	1.000	0.975	0.958	0.816
VAE[gru]_TSIS_M[768][mpl]	1.000	0.987	0.945	0.962	0.807
VAE[gru]_TSISO_M[768][mpl]	1.000	0.992	0.949	0.958	0.803
VAE[gru]_TSISR_M[768][mpl]	1.000	0.993	0.966	0.946	0.757
VAE[gru]_TSSA_S[768][mpl]	1.000	0.978	0.958	0.961	0.688
VAE[gru]_TSDY_S[768][mpl]	1.000	1.000	0.963	0.972	0.849
VAE[gru]_TSID_S[768][mpl]	1.000	0.999	0.943	0.982	0.886
VAE[gru]_TSIS_S[768][mpl]	1.000	0.991	0.932	0.979	0.860
VAE[gru]_TSISO_S[768][mpl]	1.000	0.992	0.940	0.974	0.850
VAE[gru]_TSISR_S[768][mpl]	1.000	0.990	0.941	0.973	0.852

In terms of the distribution learning benchmarks, it is observed that t-SMILES-based models, with the exception of the TSSA models, exhibit higher novelty scores than SMILES, DSMILES and SAFE based models and higher or comparable FCD scores.

The SAFE-based model exhibits the lowest valid and novelty scores among all tested models. The DSIMILES model demonstrated the second lowest validity and novelty scores, which are only better than the SAFE model.

The SELFIES-based model exhibits the lowest FCD score among all tested models, with the exception of TSSA. Furthermore, the TSDY_B, TSID_M, TSISR_M, and TSYD_S models exhibit both higher novelty and FCD scores than the SELFIES model. Given the inverse relationship between novelty and FCD scores, it is reasonable to infer that the majority of t-SMILES models would demonstrate superior performance to SELFIES on both novelty and FCD.

In comparison to BRICS and Scaffold, models based on MMPA exhibit lower FCD scores, which reflect that MMPA is more complex than the BRICS and Scaffold because the most fine-grained partitioning was used. In order to enhance the efficacy, it is advised that either larger capacity models be developed or that more extensive training procedures be implemented.

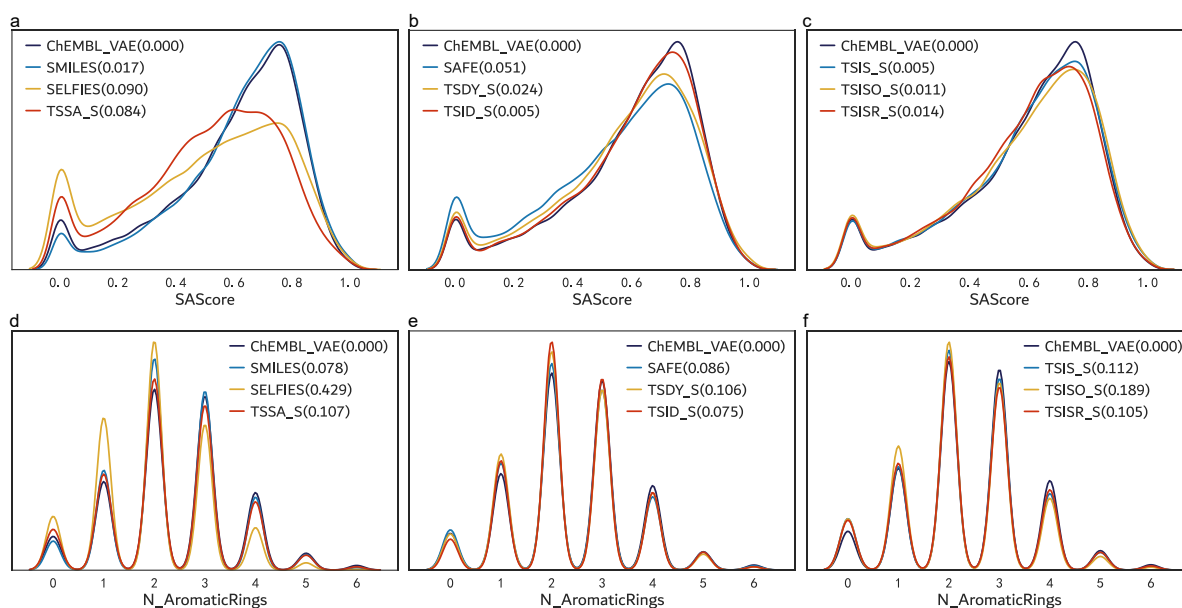


Fig.6 Physicochemical Properties on ChEMBL using VAE.

The results of the analysis of the physicochemical properties indicate that SMILE, TSDY, TSID and TSIS models demonstrate a superior fit to the training dataset in comparison to the SELFIES and SAFE models. When comparing the t-SMILES family, the TSID model exhibits the highest performance in terms of fitting accuracy, outperforming other code algorithms.

The lower FCD scores obtained by the TSSA and SELFIES models, the latter continues to yield a greater number of molecules with fewer aromatic rings. Moreover, the data illustrated in the N-MaxBondInRings figures suggests that the SELFIES-based model produces a greater

number of molecules with larger rings. Subsequently, the SAFE model is considered.

Diffusion Models on ChEMBL

The generation of realistic images is considered a primary objective in evaluating the performance of generative models. Diffusion models have emerged as the new state-of-the-art family of deep generative models. They have broken the long-time dominance of generative adversarial networks (GANs) [44] in the challenging task of image synthesis and have also shown potential in a variety of domains, ranging from computer vision, natural language processing, temporal data modeling ,multi-modal modeling, robust machine learning, to interdisciplinary applications in fields such as medical image reconstruction and computational chemistry[45]. Consequently, a published diffusion model DIFFUMOL[29],which combined a diffusion model with Transformer architecture to tokenize SMILES and generate molecules with specified scaffolds and properties, is employed for the assessment of t-SMILES codes and other LMRs in this section. Given that DSMILES exhibits relatively lower performance than SMILES and SELFIES, it will not be included in the this experiment due to the computing resources. The detailed results are summarized in Table 7 and Fig 7.

Table.7 Results for the Distribution-Learning Benchmarks on **ChEMBL** using **Diffusion** Models. Two models are trained. Larger models with 12 layers are trained on GPU: NVIDIA Tesla V100s. Smaller model with 8 layers are trained on GPU: NVIDIA GeForce RTX 3090.

Model	Valid	Unique	Novelty	KLD	FCD
DIFFUMOL[L12][29]	0.943	1.000	1.000	-	-
DIF_SMILES[L12]	0.935	0.935	0.913	0.942	0.700
DIF_SMILES[L8]	0.876	0.875	0.858	0.910	0.608
DIF_TSDY_B[L8]	1.000	0.998	0.943	0.930	0.654
DIF_TSID_B[L8]	1.000	0.998	0.937	0.944	0.723
DIF_TSIS_B[L8]	1.000	0.976	0.886	0.909	0.650

Compared to the published baseline model, DIFFUMOL[29], which is a 12-layer Transformer architecture, in this experiment, a smaller diffusion model, DIF_SMILES[L8], which is an 8-layer Transformer architecture, is trained as a baseline model for evaluation. All models based on t-SMILES use the same hyperparameters with DIF_SMILES, except for the training epochs. As anticipated, the newly trained model DIF_SMILES receives relatively lower valid, unique, and novelty scores than DIFFUMOL. Furthermore, we retained DIFFUMOL as DIF_guacamol2 using the original training data in the published paper and calculated five metrics as a reference, as KLD and FCD were not calculated by DIFFUMOL.

Firstly, the DIFFUMOL[29] model and the newly trained model, DIF_guacamol2, achieve comparable valid scores, indicating that the latter can be considered an acceptable baseline model.

When analyzing the distribution learning metrics, Table 7 reveals that a larger SMILES-based model with 12 layers has the potential to outperform a smaller model with 8 layers. However, the smaller TSID-based model exhibits considerably superior performance across all five metrics in comparison to the larger SMILES-based model. Moreover, the smaller TSDY and TSIS models demonstrate enhanced performance on the Novelty-FCD score relative to the SMILES model. These findings suggest that t-SMILES codes are more efficient than SMILES codes, as even smaller models using t-SMILES can extract more useful information than larger SMILES models.

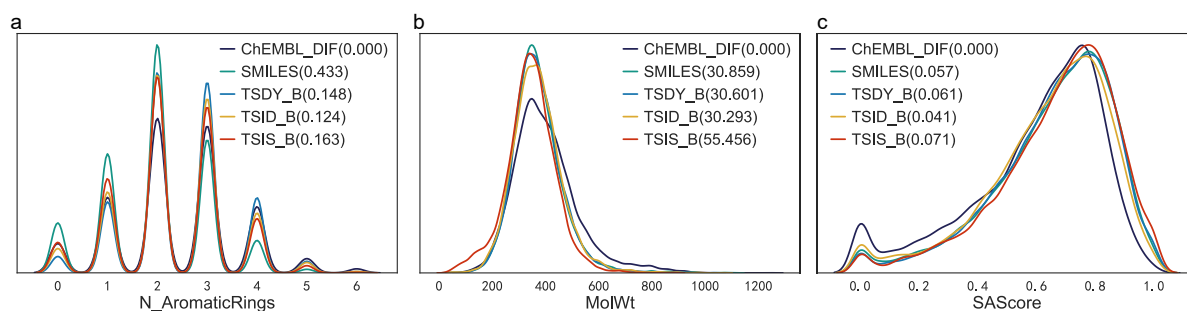


Fig.7 Physicochemical Properties on ChEMBL using diffusion model.

In evaluating the physicochemical properties, the SAScore figure indicates that t-SMILES and SMILES models achieve comparable positive results. However, the figures of MolWt reveal that both SMILES and t-SMILES models produce a pronounced Gaussian distribution, which deviates significantly from the training data. This observation aligns with the diffusion model's principle of sampling latent variables from a Gaussian distribution. Moreover, these figures also provide insight into the reason for the lower FCD scores observed.

Regarding the N-AromaticRings metric, the SMILES-based model tends to produce a higher number of molecules with fewer aromatic rings. In contrast, the t-SMILES-based model generates a greater number of molecules with a significantly higher count of aromatic rings. The SAScore figure demonstrates that both SMILES and t-SMILES models generate more molecules with better scores, suggesting that the diffusion model produces a higher quality of molecules. For a detailed comparative analysis, please refer to the discussion section.

As illustrated in Fig.8, the SMILES base model exhibits a narrow chemical space with the lowest generalizability, as indicated by the lowest Novelty-FCD scores. In contrast, the TSID-based model explores the widest chemical space with the highest generalizability, followed by TSDY and TSID.

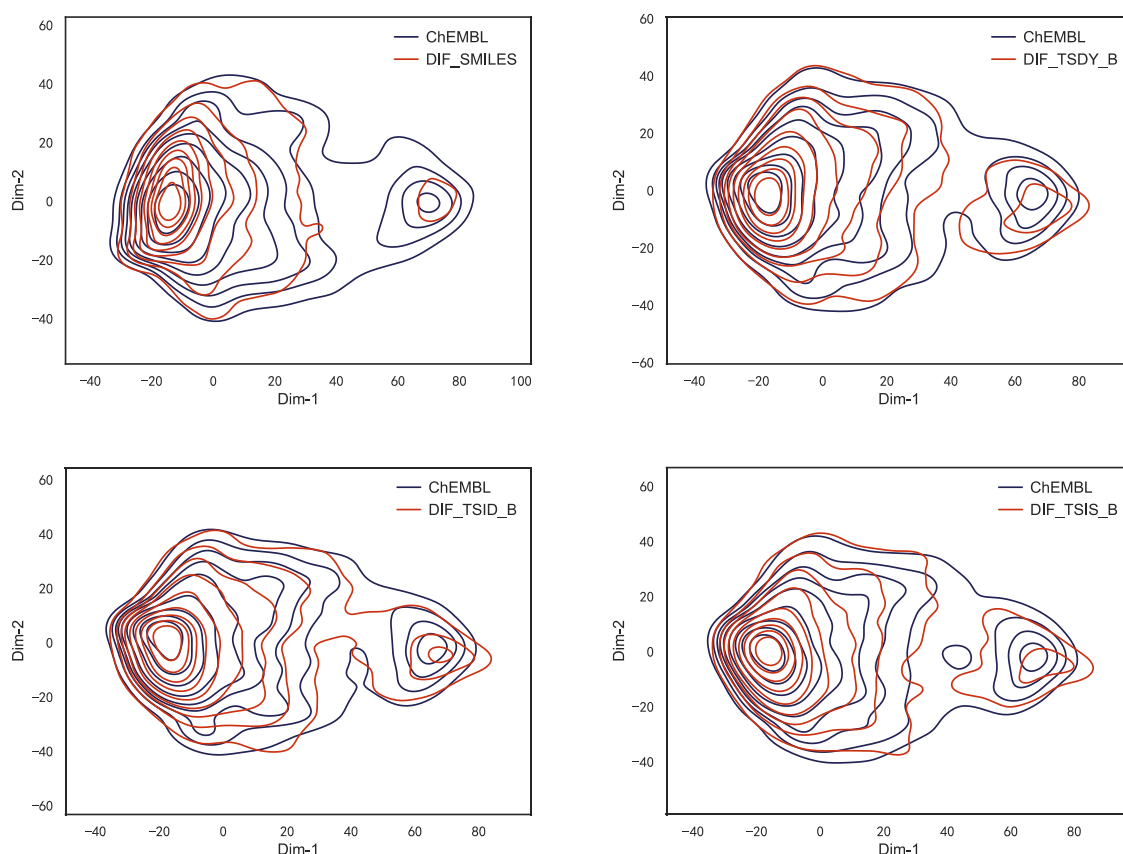


Fig.8 Visualization of the training data and the generated molecules on ChEMBL using diffusion model for different LMRs. ISOMAP[46] is used as a dimensionality reduction algorithm, RDKit topological fingerprint[19] is used as a fingerprinting algorithm.

GPT Models on Zinc and Multi-Distribution Molecules

In order to further evaluate the efficacy of t-SMILES, additional experiments were conducted on smaller molecule Zinc and a more complex dataset with multi-distributions. As demonstrated in Table 8 and Table 9, which indicates a similar result to that observed on ChEMBL.

- 1) The hidden pattern of tree structure used by t-SMILES is easily to be read, as evidenced by the score of 1.0 when calculating the percent of correct FBT.
- 2) t-SMILES models achieve higher novelty scores when the FCD score is similar to SMILES. This indicates that t-SMILES code exhibits greater generalizability.
- 3) TSISO outperforms SAFE in all calculated metrics, including syntax, distribution learning and physicochemical properties.
- 4) TSID and TSIS demonstrate a high level of fitting with the training data, comparable to that of SMILES with respect to physicochemical properties.

- 5) SAFE based models get lower scores than SMILES as well.
- 6) SELFIES models generate more molecules with less aromatic rings, indicating that the semantics of SELFIES is challenging to be learned.

Table.8 Results for the Distribution-Learning Benchmarks and LVSD on **Zinc** (about 249,000 molecules) using **GPT**. In ref[15], the standard training epochs are 50 on GPU: NVIDIA Tesla V100s, while in this experiment they are 10 on GPU: NVIDIA GeForce RTX 3090.

Model	Valid	Unique	Novelty	KLD	FCD	LVSD=0 Or Correct FBT	LVSD=2
MolGPT[40]	0.994	1.000	0.797	N/A	N/A		
SMILES[R10]	0.980	0.979	0.974	0.991	0.939	-	-
DSMILES[R10]	0.920	0.919	0.915	0.992	0.924		
SELFIES[R10]	1.000	1.000	0.996	0.978	0.881	-	-
SAFE[R10]	0.839	0.832	0.830	0.974	0.916	0.636	0.950
TSSA_B[R10]	1.000	0.969	0.967	0.973	0.731		
TSID_B[R10]	1.000	0.999	0.992	0.986	0.924	(1 wrong in 10k)	
TSIS_B[R10]	0.999	0.999	0.995	0.990	0.936	(0 wrong in 10k)	-
TSISO_B[R10]	0.999	0.998	0.991	0.988	0.935	-	-
TSISR_B[R10]	0.999	0.996	0.992	0.985	0.928	0.936	0.999
TSSA_M[R30]	1.000	0.968	0.960	0.991	0.839	-	-
TSID_M[R10]	0.999	0.999	0.996	0.977	0.912		
TSIS_M[R10]	1.000	0.999	0.996	0.990	0.933		
TSISO_M[R10]	0.999	0.997	0.992	0.991	0.933		
TSISR_M[R10]	0.999	0.997	0.995	0.987	0.929		
TSISD_M[R10]	0.999	0.997	0.995	0.981	0.913		
TSSA_S[R10]	1.000	0.984	0.984	0.970	0.816		
TSID_S[R10]	1.000	1.000	0.997	0.986	0.925		
TSIS_S[R10]	0.999	0.996	0.992	0.990	0.936		
TSISO_S[R10]	1.000	0.996	0.994	0.990	0.935		
TSISR_S[R10]	1.000	0.997	0.993	0.990	0.935		
TSISD_S[R10]	0.999	0.997	0.994	0.984	0.937		

Table 9. Results for the Distribution-Learning Benchmarks and LVSD on **Multi-distribution** tasks using **GPT**.

Model	Valid	Unique	Novelty	KLD	FCD	LVSD=0 Or Correct FBT	LVSD=2
LSTM_SM-RNN[47]	0.969	0.996	0.937	-	-	-	-
LSTM_SF-RNN[47]	1.000	0.989	0.950	-	-	-	-
SM-Transformer[48]	0.970	1.000	0.910	-	-	-	-
SF-Transformer[48]	1.000	1.000	0.980	-	-	-	-
SMILES[R30][256]	0.983	0.978	0.878	0.998	0.939	-	-
DSMILES[R30][256]	0.955	0.949	0.852	0.998	0.945		
SELFIES[R30][256]	1.000	0.997	0.930	0.988	0.888	-	-
SAFE[R30][256]	0.983	0.966	0.884	0.996	0.914	0.749	0.966
TSID_B[R30][256]	1.000	0.996	0.902	0.997	0.940	-	-
TSIS_B[R30][256]	1.000	0.996	0.896	0.998	0.948	(0 wrong in 10k)	-
TSISO_B[R30][256]	1.000	0.994	0.888	0.997	0.939	-	-
TSISR_B[R30][256]	1.000	0.994	0.887	0.997	0.942	0.968	0.999
TSISD_B[R30][256]	1.000	0.993	0.883	0.995	0.934	-	-
TSID_S[R30][256]	1.000	0.997	0.921	0.997	0.937	-	-
TSIS_S[R30][256]	1.000	0.995	0.897	0.998	0.945	-	-
TSISD_S[R30][256]	0.999	0.994	0.901	0.998	0.947	-	-

Discussion

Distinctive Properties

The t-SMILES algorithm exhibits several notable properties that distinguish it from previous LMRs. This section will examine t-SMILES in the context of some of the most significant topics in the field of deep learning.

Decomposition and Hierarchical learning

According to cognitive psychology and related disciplines, the development of complex problem-solving behaviour in biological agents depends on hierarchical cognitive mechanisms[49]. One of the core strengths of deep learning lies in its hierarchical structure and layer-wise feature extraction. This capability allows deep learning models to automatically learn and extract high-level abstract features from raw data, which is essential for many tasks that require understanding complex patterns, such as image recognition, natural language processing, and molecular generation. The efficacy of hierarchical learning ability hinges on the ability of the data to satisfy decomposability to a certain extent[26].

The concept of decomposability involves breaking down complex data into simpler components or features that models can learn and recombine at various levels of abstraction. This approach leverages the natural structure or patterns within the data. For instance, in image processing, lower layers of a model might capture basic features like edges and textures, while higher layers aggregate these features into more abstract representations such as shapes and objects.

Similarly, molecules exhibit inherent decomposability, which allows for hierarchical coding. The t-SMILES algorithm takes advantage of this by incorporating explicit hierarchical structure information into linear molecular representations using a tree-based approach. This hierarchical representation aligns with the natural decomposability of molecules, enabling more effective modeling and understanding of their complex structures.

With regard to the experimental outcomes on ChEMBL, TSIS and TSISR serve as illustrative examples due to their identical underlying models and symbols, differing only in the hierarchical structure of their sequences. This controlled setup helps eliminate potential interfering factors. Generally, TSIS consistently achieves higher FCD scores compared to TSISR. However, the results for TSIS and TSISR on Zinc do not show statistically significant differences, which can be attributed to the limited number of tree structures available due to the smaller size of the zinc molecules.

Some researchers propose that the core of representation learning is the creation of multi-level feature representations with sufficient depth[50]. Additionally, others argue that the ability to capture hierarchical information in sequential data is crucial for developing intelligent systems capable of understanding and processing language[38]. In light of these considerations, our approach may provide valuable insights that can advance the field of molecular string representations.

Compositional generalization

Human language learning enjoys a good kind of combinatorial explosion - if a person knows the meaning of “to run” and that of “slowly”, he can immediately understand what it means “to run slowly”, even if he has never uttered or heard this expression before[51]. Compositionality is the classic idea that new representations can be constructed through the combination of primitive elements[52], which enables natural languages to construct complex semantic meanings from the combinations of simpler semantic elements[53][54]. Even with just a few examples, people can learn remarkably rich conceptual models[52]. Despite a multitude of empirical studies, little consensus exists on whether neural networks are able to generalise compositionally[55][52][56][57][58][59][60].

In the t-SMILES framework, if it is assumed that deep generative models lack the capacity to perform compositional generalization, there is still the possibility of achieving this when converting t-SMILES to SMILES. It is evident that when reconstruction is performed directly on training data, compositional generalization is the underlying process. It is reasonable to anticipate that the implementation of an advanced reconstruction algorithm, such as the goal-directed method[15], would result in superior outcomes. The second level of compositional generalization for t-SMILES is based on the capacity of neural networks. If assuming that deep neural networks possess at least a limited notion of compositionality[52], it is reasonable to infer that the t-SMILES system would have compositional generalization ability from inner-fragments and inter-fragments.

In this scenario, the fragment-based t-SMILES algorithm achieves higher novelty score when getting same FCD score if model is well trained, which seems to be a more competitive linear descriptor than SMILES. An intriguing area of future research would be the investigation of the degree of compositional generalization achieved by these algorithms.

Scaling law

As prior work[61] suggested, one fundamental characteristic of LLMs is the scaling law,

which describes how the performance of LLMs improves as they scale in terms of model size, training data, and computational resources. This power-law relationship suggests that larger models trained on more data tend to capture more complex patterns and generalize better to new tasks[62][63].

As illustrated in Tables 2 and 3, models that undergo training on a greater volume of data tend to exhibit both higher novelty and FCD scores for all tested LMRs using LSTM or Transformer model. This indicates that more complex patterns have been captured when training more. Similarly, the experiments on diffusion models demonstrate that larger SMILES-based model achieves higher Novelty-FCD scores than smaller SMILES-based model.

However, larger SMILES based diffusion model obtains lower Novelty-FCD scores than smaller t-SMILES model. This implies that complex patterns may be more efficiently learned from t-SMILES code than SMILES code by this diffusion model.

Pre-trained then Fine-tuned

Recent years have featured a trend towards pre-trained language representations in NLP systems, applied in increasingly flexible and task-agnostic ways for downstream transfer. In this pattern, models are designed to be large to absorb information during pre-training, and are then fine-tuned on very narrow task distributions. There is evidence suggesting that the generalization achieved under this paradigm can be poor because the model is overly specific to the training distribution and does not generalize well outside it [64][65]. Thus, the performance of fine-tuned models on specific benchmarks, even when it is nominally at human-level, may exaggerate actual performance on the underlying task[66][67]. So the research[68] findings indicate a preference for few-shot learning over the necessity of explicit fine-tuning.

The pretrained then fine-tuned paradigm represents a classical scenario in the context of chemistry and material science applications, where the availability of experimental data is inherently limited[69]. It is therefore anticipated that meaningful results can be obtained with tens to hundreds of data points. The preceding study[15] on the low-resource dataset demonstrated that even a singleton TSSA-based model with reconstruction as augmentation achieved superior results compared to a pre-trained then fine-tuned model on SMILES. This result is primarily attributable to the distinctive logic of t-SMILES, which enables t-SMILES code to demonstrate a high degree of compositional generalization ability.

Multimodal Large Models (MLMs)

MLMs are becoming a significant research focus, combining powerful large language models with multimodal learning to perform complex tasks across different data modalities[70]. MLLMs represent a significant advancement in AI by extending the capabilities of traditional LLMs to process and analyze multiple modalities. MLLMs can solve complex real-world problems that require understanding and reasoning across different types of information[71].

As indicated by the results of a prior study, the pretraining of larger models does not appear to enhance out-of-distribution (OOD) generalization in natural language processing (NLP), which is inconsistent with findings from computer vision. However, the pretraining of models on diverse data does demonstrate an improvement in OOD generalization[60].

The t-SMILES algorithm enables the creation of multi-language system, as evidenced by a previous study[15] which demonstrated enhanced performance using hybrid data. A potential avenue for future research is to investigate whether this diversity is beneficial for few-shot learning and out-of-distribution generalization for property prediction tasks.

Comparison of CLMs and LMRs

The capability of different CLMs

Generative deep learning is reshaping drug design. CLMs, which generate molecules in the form of molecular strings, bear particular promise for this endeavor. Evaluation frequently functions as a catalyst for progress, a benchmark for tracking this progress, and a window into the criteria deemed important in a field. Quantitative measurements provide methods not only for constructing a relative record of this progress, but also for illuminating the value of recent breakthroughs in relation to previous ones.

The diverse architectures of CLMs play a crucial role in determining the model's efficiency. Given that the tested models have been evaluated as being at the cutting edge of their respective fields, a comprehensive assessment of their overall performance is both pertinent and essential. This evaluation will provide insights into the strengths and limitations of each model, ensuring that the most effective architecture is identified for specific tasks.

A comparative evaluation was conducted between four different types of CLMs, comprising two autoregressive models (LSTM and GPT) and two latent variable models (VAE and diffusion model), as illustrated in Fig.9 and Fig.10.

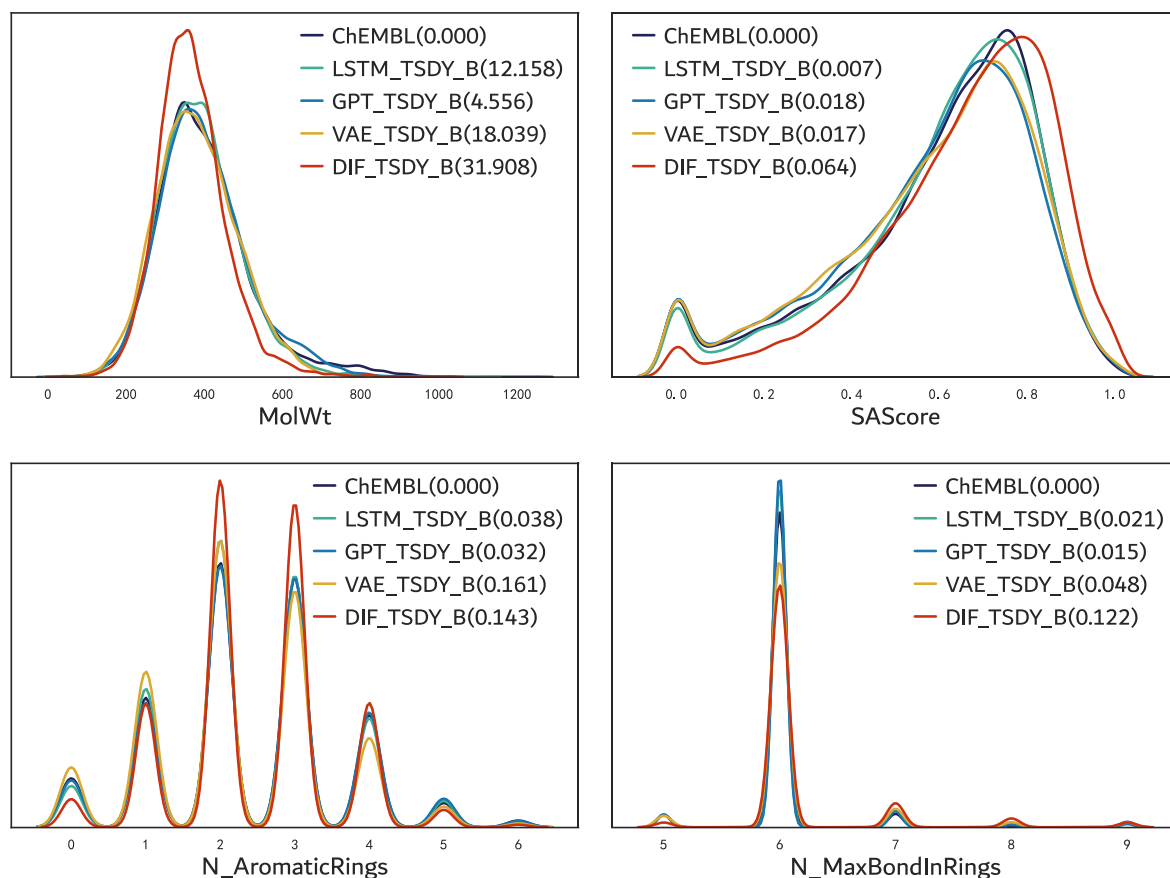


Fig.9 Physicochemical Properties on **ChEMBL** using diffusion model for different CLMs.

In general, GPT models consistently achieve the highest FCD-Novelty scores, whereas diffusion models tend to achieve the lowest FCD scores and require longer training times.

The evaluated LSTM model demonstrates syntactic learning capabilities similar to those of the GPT model, effectively learning the tree structure in t-SMILES and the order in both t-SMILES and SAFE, much like the GPT model. However, LSTM models exhibited relatively weaker performance in learning complex structure and semantic information compared to GPT models. Furthermore, LSTM models produce molecules with a smaller MolWT than GPT models. Additionally, a ten-round LSTM model did not achieve the performance of a single-round GPT model. As a result, LSTM models generally demonstrated lower performance compared to GPT models across all LMRs.

The evaluated VAE model shows a comparable ability to learn grammar and semantics. The curves for MolWT and SAScore indicate a high degree of fit to the training data. However, the N-AromaticRings and N_MaxBondInRing models outperform the diffusion model but still produce the least favorable results among the four models. This suggests that the tested GRU based VAE model generates molecules with fewer and smaller rings. Future studies could

explore whether a Transformer-based VAE model might achieve better performance.

In the context of the diffusion model, it is clear that it stands apart from the other models based on the comparative analysis results. The diffusion model shows a comparable novelty score but achieves the lowest FCD scores across all LMRs. It also generates a higher number of molecules with relatively low MolWT, which significantly deviates from the training data distribution. Despite this, it outperforms all other models in terms of SAScore. This superior SAScore performance may be partly due to the smaller number of molecules in the training data with poor SAScore.

Informally, generalizations within the training space can be viewed as interpolations, while generalizations outside the training space are considered extrapolations[72]. As illustrated in Fig. 10, both VAE and diffusion models exhibit strong interpolation capabilities, as evidenced by the generated molecules positioned between two curves of training data. In contrast, LSTM and GPT models align more closely with the distribution of the training set but show slightly weaker performance in interpolation compared to VAE and diffusion models. All models, however, demonstrate limited extrapolation abilities. Notably, the curves of SMILES are encompassed by the curves of TSDY_B.

One issue that requires further investigation is that the GRU architecture by the VAE model encounters comparable challenges to those faced by LSTM in parsing complex structures and long-range dependencies within a sequence. The superior interpolation capabilities of the VAE model are primarily attributed to the superior characteristics of the VAE architecture or the suboptimal performance of the GRU.

Further exploration of advanced architectural designs could enhance performance related to the foundational algorithmic logic of diffusion models. Additionally, one significant challenge in AI-assisted molecular discovery is the preparation of data, which frequently involves low-resource and non-Gaussian distributions, as highlighted by the TARTARUS benchmark[73]. Addressing these issues presents an opportunity for future research. For a thorough understanding of the theoretical foundations and summaries of diffusion models, please consult references [74] and [75].

The field of generative modeling is undergoing rapid development and innovation, with various models showcasing different strengths and weaknesses for de novo molecule design. While Transformer architectures are renowned for their superior performance and adaptability, they face challenges related to computational complexity and memory limitations as model

size and application requirements increase.

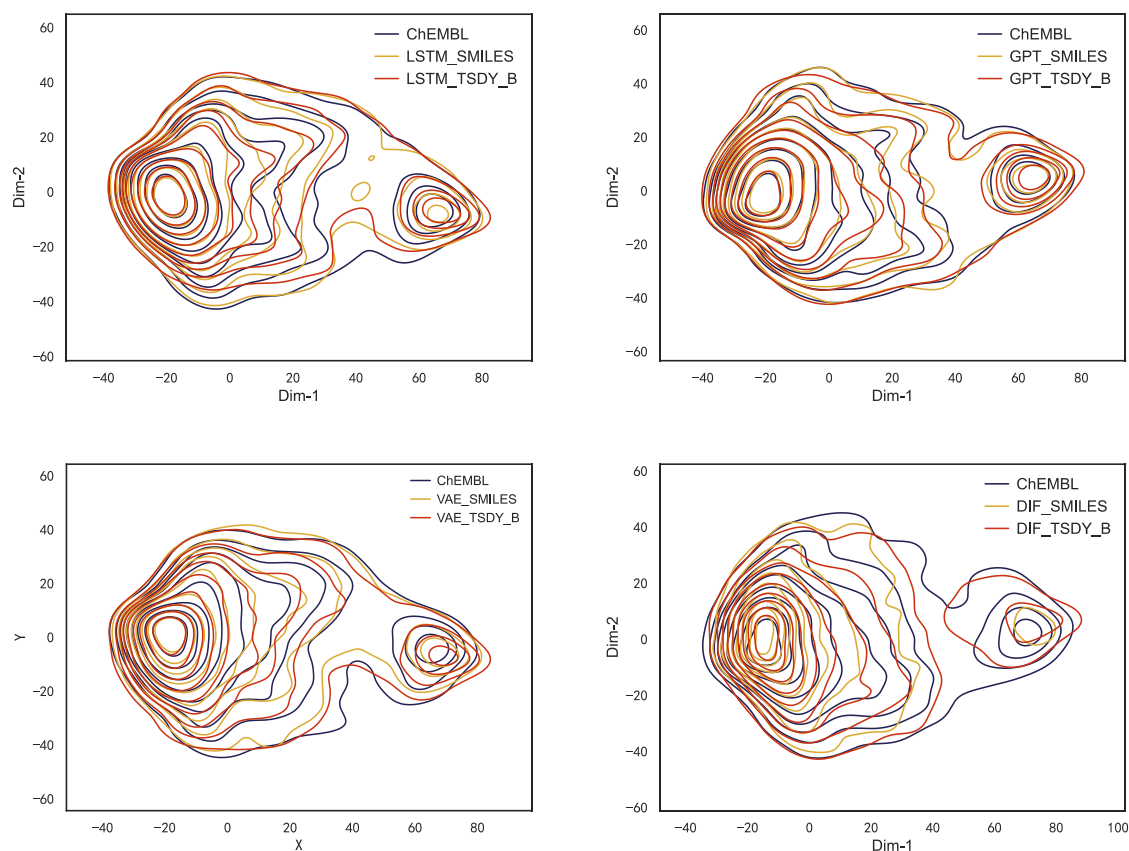


Fig.10 Visualization of the training data and the generated molecules on ChEMBL using VAE model for different LMRs. ISOMAP[46] is used as a dimensionality reduction algorithm, RDKit topological fingerprint[19] is used as a fingerprinting algorithm. On the left of each panel, there are eight small contour circles representing ChEMBL. On the right of each panel, there are three additional small contour circles. All 11 smaller circles are enclosed within a single larger contour circle.

LSTM: SMILES: left-8, right: 3; TSDY_B: left-8, right: 3; the outermost contour: yes.

GPT: SMILES: left-8, right: 3; TSDY_B: left-8, right: 4; the outermost contour: yes.

VAE: SMILES: left-8, right: 2; TSDY_B: left-8, right: 3; the outermost contour: yes.

DIF: SMILES: left-9, right: 1; TSDY_B: left-9, right: 2; the outermost contour: no

Other models, such as Generative Adversarial Networks (GANs)[44][74], Normalizing Flows[75], and Genetic Algorithms (GA), also present valuable approaches but are not covered extensively in this context due to the length of the studies. These alternative models could provide interesting avenues for further research.

Additionally, although Transformer models have demonstrated the best comparative performance, emerging models like xLSTM[76] and S4[77] also exhibit promising potential and merit exploration, it will be a promising direction for future work.

The capability of different LMRs

SMILES vs t-SMILES

The t-SMILES framework has the ability to unify classical SMILES as TS_Vanilla, making t-SMILES a superset of SMILES[15]. Although SMILES is still used to represent molecular substructure, t-SMILES cuts molecules into small pieces and abandons the algorithm of depth-first traversal of molecular trees, which fundamentally reduces the depth of nesting and the proportion of characters that must appear in pairs.

The concept of t-SMILES algorithm involves breaking down large problems into smaller and levels, each addressing sub-tasks at different levels of abstraction. This approach simplifies the overall problem-solving process. Additionally, as demonstrated by previous experiments and analyses, the hierarchical structure inherent in the t-SMILES algorithm not only facilitates learning but also provides a more detailed and comprehensive representation of the information.

SELFIES vs Others

The representation of molecules in SELFIES employs a wholly distinct approach. A comparative analysis of models based on SELFIES and those based on SMILES and t-SMILES, as well as evaluations of CLMs employing LSTM, GPT, and VAE approaches, indicates that models based on SELFIES exhibit comparatively lower performance.

The relatively low scores observed in SELFIES models can be attributed to their tendency to generate molecules with fewer aromatic rings, which presents a challenge in learning the semantics. In other words, SELFIES models may produce more novel molecules if the similarity to the training data is disregarded. This observation is also consistent with the findings of other researchers, such as those reported in ref[78]. With regard to the limitations of SELFIES, a recent study suggested that learning the complete removal of valency constraints, which the researcher designated "unconstrained SELFIES," has been demonstrated to enhance performance outcomes[79].

SAFE vs t-SMILES

When comparing the algorithms of SAFE and t-SMILES, three perspectives become apparent:

1. Paired numbers can be divided into two categories.

The first category is the numbers that denote ring breaks in the classical SMILES grammar, and the second category is the numbers that denote cut points. The SAFE algorithm combines these two categories into one, which creates a semantic challenge. Nevertheless, the model

must still learn and classify them.

2. Matching and dependency of paired numbers

The dependency length of the first type of number in TSID is limited within the fragment. Additionally, the dependency length of the second type of number [n*] can span across fragments. It is important to note that SAFE does not categorize the numbers, Therefore, the matching lengths and dependency lengths of the numbers can be interpreted as whole strings. Because SAFE is longer than SMILES, resulting in longer grammar dependencies in SAFE than in SMILES. It is worth noting that in both SAFE and TSID, the matching range of parentheses is limited to one fragment. So, in summary, SAFE does not address the long dependencies in SMILES syntax and may even increase the difficulty. For Example:

- 1) c1³cc(F)c(O)c(C2=CCc³c-2c(C)nn2C)c1.CO³ : Error: three symbols '3' that should be in pairs.
- 2) 'N15CCC³CCC1)CCCO².Cc1cccc4c15.c16ccc7o1.C³6=O.C7(F)F.N³4': Error: unpaired symbols: ')', '2' and '3'.
- 3) 'c1^{%18}c[nH]c2cccc12.c1⁷ncc(Cl)c^{%10}n1.N16CCCC9C1.C56=O.CC⁷.N⁵7.N⁸9': Error: unpaired symbols: '%18', '%10', '7', and '8'.

3. Molecule tree and sorting fragments based on size

Both foundational patterns can be learned by deep learning models. Sorting fragments based on size in SAFE may increase long-term dependencies. For example:

SMILES:

CCCCC1C(=O)N(C(C2SCCCS2)C2OC(C)(C)OC2C2COC(C)(C)O2)C1C(C)=Cc1cccc1

The length of the string is 67.

SAFE:

C1⁶OC(C)(C)OC1C1COC(C)(C)O1.C17C(=O)N4C1C=3C.C=3c1cccc1.C15SCCCS1.CCCC7.C45⁶

The length of the string is 77, which means that the dependency of the symbol '6' becomes longer.

t-SMILES family

The t-SMILES family has been expanded to include four major categories of codes: TSSA, TSDY, TSID, and TSIS. The TSIS code can be easily expanded to TSISD, TSISO, and TSISR through the application of straightforward rules. These seven types of code will be discussed from two perspectives: the complexity of the algorithms used and the determinacy of the information conveyed.

In consideration of the degree of complexity of code algorithms, TSSA is the most

complex, employing shared atoms to link two parts. This can be evidenced by the observation that all TSSA-based models receive the lowest FCD scores across the entire t-SMILES family. TSDY and TSID are the next most complex, followed by all TSIS, including its variants, which are the simplest in comparison to the other three types of code.

- 1) TSSA vs TSDY and TSID: The distinction between the two lies in the inclusion of additional uncertainty information within the TSSA code. To illustrate, if the link point is designated as "C-N," then all atom C in one sug-fragment and all atom N in another are potential candidates for the linking point, thereby enhancing the possibility of producing novel molecules. However, parsing TSSA code is relatively more challenging than TSDY and TSID (lower FCD scores in experiment results). This indicates that either a more comprehensive model or longer training is necessary.
- 2) TSDY vs TSID: From the visualization in the diffusion model, it is apparent that the curve of TSID is covered by TSDY. A comparison of the metrics reveals that the TSDY model exhibits higher novelty and lower FCD scores than the TSID model. The distinction between TSDY and TSID can be attributed to the inclusion of more definitive information within TSID, derived from the linking token "[n*]". This observation prompts the thought that whether this difference is the primary reason that TSID is more efficiently learned than TSDY with a higher FCD score, but TSDY produces a greater number of novelty molecules.
- 3) TSIS vs TSID: The distinction between TSIS and TSID hinges on the FBT structure, which introduces a greater degree of definitive information within TSID. As illustrated in the syntax section, FBT is not an obstacle but may, in fact, be a beneficial element. However, there is no obvious statistical difference between the two that can be observed from the experimental results on ChEMBL and Zinc.
- 4) TSIS vs TSISR: The distinction between TSIS and TSISR is that TSIS uses the BFS algorithm to parse AMT, whereas TSISR randomly sorts sub-fragments. However, the TSISR models consistently exhibit the lowest FCD scores across all CLMS on ChEMBL. This finding suggests that incorporating hidden hierarchical and deterministic information can improve the effectiveness of linear molecular representations. By capturing underlying structural relationships, models can better represent and process molecular data, leading to enhanced performance in various tasks.

In conclusion, for smaller molecules such as those in Zinc, no significant statistical distinction can be observed between TSID, TSIS and its variants. One of reason is that the AMT and FBT are simply for the powerful large transformer models.

For larger molecules, such as those in ChEMBL, hierarchical information is essential for effective data analysis and interpretation. Specifically, TSIS may achieve performance comparable to TSID. However, among the TSIS variants, TSISR remains the most challenging. Nevertheless, based on the scaling law[61] and experimental results on Zinc, increasing model capacity, augmenting training data, or extending training epochs could potentially enhance the performance of the TSIS code.

The experimental results and subsequent discussion suggest that TSSA is the optimal choice for goal-directed tasks due to its ability to avoid "striking similarity" to the training dataset while achieving good novelty with reasonable similarity. TSDY is a balanced method suitable for both goal-oriented and distributional reproduction tasks. For distribution reproduction experiments, TSIS and TSID are recommended as they effectively align with the physicochemical properties of the training data.

Limitations

Correction process in t-SMILES algorithm

Despite the shorter length of the sub-fragment in t-SMILES compared to SMILES on average, as well as the reduced long-decency, the t-SMILES algorithm uses specific correction processes to guarantee the solution is robust.

1. If a sub-fragment is unable to be parsed as a valid fragment-mol, a fragment from the dictionary that is the most similar to the invalid sub-fragment is selected as a replacement.
2. If the link points [n*] in the TSID and TSIS code are unable to be correctly matched, the TSDY style is used as a corrective measure.
3. If all nodes of FBT or AMT could not be assembled as a single molecule due to the assembled graph conflicting with chemical knowledge, some smaller sub-fragments would be discarded, though this scenario is an infrequent occurrence when the model is adequately trained.

Hallucination of LLMs in chemistry

It has been observed that LLM models encounter difficulties in comprehending and interpreting SMILES correctly[78][80]. This may result in the generation of chemically valid molecules that are in violation of chemical principles. These findings highlight the limitations of the current evaluation metrics and emphasize the necessity for the development of chemistry-specific metrics, as the commonly used metrics are still employed for the evaluation of all models in our work.

In practice, measures such as introducing discriminative filters, integrating chemical rules, implementing multi-objective optimization, and conducting data augmentation can be employed effectively to improve the performance and reduce the risk of generating molecules that do not conform to chemical knowledge.

Hyperparameter Optimization

In this paper, rather than pursuing SOTA performance, we aim to evaluate capabilities of different LMRs in a wide range of tasks. To this end, we leverage published SOTA models that were optimized for SMILES as a foundation to assess other LMRs with minimal hyperparameter updates, such as training epochs. Consequently, in practice, the hyperparameters should be optimized for each individual LMR to achieve SOTA performance.

Conclusion

In this study, we introduced a novel algorithm, TSIS, and its variants to the t-SMILES family. Through a systematic experimentation process involving different LMRs and different CLMs, we demonstrated that the hierarchical structures of t-SMILES enhance the generalization ability of linear molecular representations by providing a more organized and comprehensive way to capture and utilize patterns within the data. This structure allows models to better understand and apply relationships at different levels of abstraction, improving their ability to generalize beyond the training set.

To be specific, the hierarchical structure of TSIS and TSID is straightforward to learn. SAFE is the most challenging code to be analyzed due to its long-term dependency. Furthermore, the SELFIE has been observed to consistently yield a greater number of molecules with larger rings due to its inherent logical.

With respect to the distribution learning metrics, TSIS demonstrates performance that is comparable to TSID. However, TSISR stands out as the most challenging variant of TSIS to analyze, requiring more intricate methods to achieve optimal results.

In the context of generative models, GPT has proven to be the most effective in achieving the highest scores for Novelty-FCD, indicating its strong capability to generate novel and diverse outputs while maintaining a high degree of fidelity to the desired characteristics. The VAE and diffusion models exhibit strong capabilities in interpolation, allowing them to generate outputs that smoothly transition between known data points. This ability to interpolate effectively makes these models valuable for tasks that require generating diverse yet coherent outputs within the learned data distribution.

The tested diffusion model demonstrates a higher sensitivity to distributions than other models, representing a promising avenue of future investigation. Addressing the challenge of chemical domain-specific low-resource problems is an important direction for future research.

This is the second study on t-SMILES, aiming to further complete its understanding. Future research could explore interpretability, properties, retrosynthesis and reaction prediction, materials science, and other related fields. Additionally, the core algorithm of t-SMILES could be implemented in a faster programming language, such as C++, to enhance performance.

Methods

The hyperparameters of the utilized models keep identical to those utilized in previous research.

1. The evaluated LSTM model was published in GuacaMol[43] and MOSES[42], which is a 3-layer architecture.
2. The evaluated GPT model was published in MolGPT[40], which is a 8-layer Transformer architecture.
3. The evaluated VAE model was published in GuacaMol[43] and MOSES[42], which is based on 3-layer GRU architecture.
4. The evaluated Diffusion model was published in DIFFUMOL[29], which is based on 12-layer Transformer architecture.

In this study, three GPUs: NVIDIA Tesla V100s, NVIDIA GeForce RTX 3090 and NVIDIA Quadro RTX4000 are used to train deep learning models. The encoding and decoding of t-SMILES string can be performed on a CPU without the need for a GPU.

Dataset: The models are evaluated on two publicly available datasets, ChEMBL-21[81] and Zinc[82], which are the same as the dataset used in the previous t-SMILES paper[15]. For the sake of universality, a subset of ChEMBL-21 with SMILES character length less than 120 is selected in this study. The molecular weight of Zinc in this study: max = 500, mean is 332. The molecular weight of ChEMBL in this study: max = 1244, mean is 400.

In addition, the molecules in the training dataset with multi-distribution come from:

- a. GDB13[83] molecules with molecular weight (MW) ≤ 185 ,
- b. ZINC[41][84] molecules with $185 \leq \text{MW} \leq 425$,
- c. Harvard clean energy project (CEP)[85] molecules with $460 \leq \text{MW} \leq 600$,
- d. POLYMERS[86] molecules with $\text{MW} > 600$.

Metrics: Distribution Learning assessed the ability of the generator to match the reference chemical space distribution in newly generated compounds. We use five benchmarks proposed by GuacaMol: validity (\uparrow), uniqueness (\uparrow), novelty (\uparrow), KL divergence (KLD) (\uparrow)[87] and Fréchet ChemNet Distance(FCD)[88] score (\uparrow) to evaluate the general performance of the model.

The Levenshtein distance (LVSD) is a similarity measure that can be used to find strings that are close to a given one. It is calculated using the minimum edit distance, which considers the number of insertions, deletions, and substitutions needed to transform one string into the other. For example, the Levenshtein distance (LVSD) of the string [29, 25, 13, 9, 6] is 0, while the LVSD of the string [22, 23, 13, 10, 9] is 2.

In addition, the number of aromatic rings in the molecule(N_AromaticRings) is used to mainly evaluate semantics. SA score(SAS)[89] is used to evaluate whether the generative models could effectively learn the physical and chemical properties of the molecules in the training set, thereby comprehensively evaluating the performance of the generative model from the perspective of distributed learning knowledge.

Conflicts of Interest

The authors declare that they have no competing interests.

Author Contributions

Juanni Wu and Ruqin Yu designed the study and manuscript. As the main designer of the project, Juanni Wu conceived the project, constructed the algorithms and Python script, performed the experiments, informatics analyses, and wrote the draft manuscript. Tong Wang, Lijuan Tang and Hailong Wu participated in the discussion and funding acquisition. All authors contributed to manuscript editing, revising and have approved the final version of the manuscript.

Acknowledgements

This research was funded by the National Natural Science Foundation of China.

Data availability

The datasets used in this study are publicly available. The processed data used in this study can be found at: <https://github.com/juanniwu/t-SMILES/>

Code availability

Code, training and generation scripts for this work can be found at: <https://github.com/juanniwu/t-SMILES/>

Reference

- [1] J. Jiménez-Luna, F. Grisoni, and G. Schneider, 'Drug discovery with explainable artificial intelligence', *Nat. Mach. Intell.*, vol. 2, no. 10, pp. 573–584, 2020, doi: 10.1038/s42256-020-00236-4.
- [2] R. Todeschini and V. Consonni, *Handbook of Molecular Descriptors*, vol. 11. Wiley, 2000. doi: 10.1002/9783527613106.
- [3] S. Raghunathan and U. D. Priyakumar, 'Molecular representations for machine learning applications in chemistry', *Int. J. Quantum Chem.*, vol. 122, no. 7, pp. 1–21, 2022, doi: 10.1002/qua.26870.
- [4] D. S. Wigh, J. M. Goodman, and A. A. Lapkin, 'A review of molecular representation in the age of machine learning', *Wiley Interdiscip. Rev. Comput. Mol. Sci.*, vol. 12, no. 5, p. null, 2022, doi: 10.1002/wcms.1603.
- [5] L. David, A. Thakkar, R. Mercado, and O. Engkvist, 'Molecular representations in AI-driven drug discovery: a review and practical guide', *J. Cheminform.*, vol. 12, no. 1, Sep. 2020, doi: 10.1186/S13321-020-00460-5.
- [6] H. Kim, E. Kim, I. Lee, B. Bae, M. Park, and H. Nam, 'Artificial Intelligence in Drug Discovery : A Comprehensive Review of Data-driven and Machine Learning Approaches', vol. 930, pp. 895–930, 2020, doi: 10.1007/s12257-020-0049-y.
- [7] K. Atz, F. Grisoni, and G. Schneider, 'Geometric deep learning on molecular representations', *Nat. Mach. Intell.*, vol. 3, no. 12, pp. 1023–1032, 2021, doi: 10.1038/s42256-021-00418-8.
- [8] H. Öztürk, A. Özgür, P. Schwaller, T. Laino, and E. Ozkirimli, 'Exploring chemical space using natural language processing methodologies for drug discovery', *Drug Discov. Today*, vol. 25, no. 4, pp. 689–705, 2020, doi: 10.1016/j.drudis.2020.01.020.
- [9] A. Cadeddu, E. K. Wylie, J. Jurczak, M. Wampler-Doty, and B. A. Grzybowski, 'Organic chemistry as a language and the implications of chemical linguistics for structural and retrosynthetic analyses', *Angew. Chemie Int. Ed.*, vol. 53, no. 31, pp. 8108–8112, 2014.
- [10] D. Weininger, 'SMILES, a Chemical Language and Information System: 1: Introduction to Methodology and Encoding Rules', *J. Chem. Inf. Comput. Sci.*, vol. 28, no. 1, pp. 31–36, Feb. 1988, doi: 10.1021/ci00057a005.
- [11] N. M. O'Boyle and A. Dalke, 'DeepSMILES: An adaptation of SMILES for use in machine-learning of chemical structures', *ChemRxiv*, Sep. 2018, Accessed: Mar. 13, 2022. [Online]. Available: <https://chemrxiv.org/engage/chemrxiv/article-details/60c73ed6567dfe7e5fec388d>
- [12] M. Krenn, F. Häse, A. K. Nigam, P. Friederich, and A. Aspuru-Guzik, 'Self-referencing embedded strings (SELFIES): A 100% robust molecular string representation', *Mach. Learn. Sci. Technol.*, vol. 1, no. 4, p. 045024, 2020, doi: 10.1088/2632-2153/aba947.
- [13] J. Arús-Pous *et al.*, 'Randomized SMILES strings improve the quality of molecular generative models', *J. Cheminform.*, vol. 11, no. 1, pp. 1–13, 2019, doi: 10.1186/s13321-019-0393-0.
- [14] M. Krenn *et al.*, 'SELFIES and the future of molecular string representations', *Patterns*, vol. 3, no. 10, p. 100588, 2022, doi: 10.1016/j.patter.2022.100588.
- [15] J. N. Wu, T. Wang, Y. Chen, L. J. Tang, H. L. Wu, and R. Q. Yu, 't-SMILES: a fragment-based molecular representation framework for de novo ligand design', *Nat. Commun.*, vol. 15, no. 1, pp. 1–15, Jun. 2024, doi: 10.1038/s41467-024-49388-6.
- [16] E. Noutahi, C. Gabellini, M. Craig, J. S. C. Lim, and P. Tossou, 'Gotta be SAFE: a new framework for molecular design', *Digit. Discov.*, vol. 3, no. 4, pp. 796–804, Oct. 2024, doi: 10.1039/d4dd00019f.
- [17] A. H. Cheng, A. Cai, S. Miret, G. Malkomes, M. Phielipp, and A. Aspuru-Guzik, 'Group SELFIES: a robust fragment-based molecular string representation', *Digit. Discov.*, vol. 2, no. 3, pp. 748–758, 2023, doi: 10.1039/d3dd00012e.
- [18] ChemAxon, 'Chemaxon Extended SMILES and SMARTS - CXSMILES and CXSMARTS', <https://docs.chemaxon.com/Display/Docs/Chemaxon-Extended-Smiles-and-Smarts-Cxsmiles-and-Cxsmarts.Md>. <https://docs.chemaxon.com/display/docs/chemaxon-extended-smiles-and-smarts-cxsmiles-and-cxsmarts.md> (accessed Jan. 31, 2024).
- [19] G. Landrum, 'RDKit : A software suite for cheminformatics , computational chemistry , and predictive modeling', *RDKit A Softw. Suite Cheminformatics, Comput. Chem. Predict. Model.*, 2013.
- [20] A. Vaswani *et al.*, 'Attention is all you need', in *Advances in Neural Information Processing Systems*, Jun. 2017, vol. 2017-Decem, pp. 5999–6009. [Online]. Available: <https://www.semanticscholar.org/paper/204e3073870fae3d05bcbcb2f6a8e263d9b72e776>
- [21] P. Dufter, M. Schmitt, and H. Schütze, 'Position Information in Transformers: An Overview', *Comput. Linguist.*, vol. 48, no. 3, pp. 733–763, Sep. 2022, doi: 10.1162/coli_a_00445.
- [22] B. Wang *et al.*, 'On Position Embeddings in Bert', *ICLR 2021 - 9th Int. Conf. Learn. Represent.*, 2021.
- [23] A. Wang, A. Singh, J. Michael, F. Hill, O. Levy, and S. R. Bowman, 'GLUE: A Multi-Task Benchmark and Analysis Platform for Natural Language Understanding', *EMNLP 2018 - 2018 EMNLP Work. BlackboxNLP Anal. Interpret. Neural Networks NLP, Proc. 1st Work.*, pp. 353–355, 2018, doi: 10.18653/v1/W18-5446.
- [24] M. Abdou, V. Ravishankar, A. Kulmizev, and A. Søgaard, 'Word Order Does Matter (And Shuffled Language Models Know It)', *Proc. Annu. Meet. Assoc. Comput. Linguist.*, vol. 1, pp. 6907–6919, 2022, doi: 10.18653/v1/2022.acl-long.476.
- [25] S. Hochreiter and J. Schmidhuber, 'Long Short-Term Memory', *Neural Comput.*, vol. 9, no. 8, pp. 1735–1780, 1997, doi: 10.1162/neco.1997.9.8.1735.
- [26] S. Ma, J. P. Long, and R. K. Bhatnagar, 'Hierarchical Learning: Theory with Applications in Speech and Vision', *J.*

- Pharmacol. Exp. Ther.*, vol. 261, no. 3, pp. 1187–1194, 1992, [Online]. Available: http://cbcl.mit.edu/publications/theses/thesis_bouvrie_2009.pdf
- [27] P. Vincent, H. Larochelle, I. Lajoie, Y. Bengio, and P. A. Manzagol, ‘Stacked denoising autoencoders: Learning Useful Representations in a Deep Network with a Local Denoising Criterion’, *J. Mach. Learn. Res.*, vol. 11, pp. 3371–3408, 2010, [Online]. Available: <https://www.semanticscholar.org/paper/e2b7f37cd97a7907b1b8a41138721ed06a0b76cd>
- [28] D. P. Kingma and M. Welling, ‘Auto-Encoding Variational Bayes’, *2nd Int. Conf. Learn. Represent. ICLR 2014 - Conf. Track Proc.*, Dec. 2013, doi: 10.61603/ceas.v2i1.33.
- [29] X. Peng and F. Zhu, ‘Hitting stride by degrees: Fine grained molecular generation via diffusion model’, *Expert Syst. Appl.*, vol. 244, no. July 2023, 2024, doi: 10.1016/j.eswa.2023.122949.
- [30] Y. Yoshikai, T. Mizuno, S. Nemoto, and H. Kusuhara, ‘Difficulty in chirality recognition for Transformer architectures learning chemical structures from string representations’, *Nat. Commun.*, vol. 15, no. 1, p. 1197, Feb. 2024, doi: 10.1038/s41467-024-45102-8.
- [31] C. A. James, ‘OpenSMILES specification’, 2007. <http://opensmiles.org/opensmiles.html> (accessed May 22, 2024).
- [32] T. A. Chang and B. K. Bergen, ‘Language Model Behavior: A Comprehensive Survey’, *Comput. Linguist.*, vol. 50, no. 1, pp. 1–58, Mar. 2024, doi: 10.1162/coli_a_00492.
- [33] Y. Zhang, A. Warstadt, H. S. Li, and S. R. Bowman, ‘When do you need billions of words of pretraining data?’, *ACL-IJCNLP 2021 - 59th Annu. Meet. Assoc. Comput. Linguist. 11th Int. Jt. Conf. Nat. Lang. Process. Proc. Conf.*, pp. 1112–1125, Nov. 2021, doi: 10.18653/v1/2021.acl-long.90.
- [34] L. Z. Liu, Y. Wang, J. Kasai, H. Hajishirzi, and N. A. Smith, ‘Probing Across Time: What Does RoBERTa Know and When?’, *Find. Assoc. Comput. Linguist. Find. ACL EMNLP 2021*, pp. 820–842, Apr. 2021, doi: 10.18653/v1/2021.findings-emnlp.71.
- [35] K. Gulordava, P. Bojanowski, E. Grave, T. Linzen, and M. Baroni, ‘Colorless green recurrent networks dream hierarchically’, *NAACL HLT 2018 - 2018 Conf. North Am. Chapter Assoc. Comput. Linguist. Hum. Lang. Technol. - Proc. Conf.*, vol. 1, pp. 1195–1205, 2018, doi: 10.18653/v1/n18-1108.
- [36] Y. Goldberg, ‘Assessing BERT’s Syntactic Abilities’, *ArXiv*, vol. 1901.05287, 2019, [Online]. Available: <http://arxiv.org/abs/1901.05287>
- [37] Y. Lin, Y. C. Tan, and R. Frank, ‘Open Sesame: Getting inside BERT’s Linguistic Knowledge’, *ArXiv*, vol. abs/1906.0, pp. 241–253, 2019, doi: 10.18653/v1/w19-4825.
- [38] K. Tran, A. Bisazza, and C. Monz, ‘The importance of being recurrent for modeling hierarchical structure’, *Proc. 2018 Conf. Empir. Methods Nat. Lang. Process. EMNLP 2018*, no. 2017, pp. 4731–4736, 2018, doi: 10.18653/v1/d18-1503.
- [39] T. Wolf, ‘Some additional experiments extending the tech report “Assessing BERT’s Syntactic Abilities” by Yoav Goldberg’, 2019.
- [40] V. Bagal, R. Aggarwal, P. K. Vinod, and U. D. Priyakumar, ‘MolGPT: Molecular Generation Using a Transformer-Decoder Model’, *J. Chem. Inf. Model.*, vol. 62, pp. 2064–2076, Oct. 2021, doi: 10.1021/acs.jcim.1c00600.
- [41] R. Gómez-Bombarelli *et al.*, ‘Automatic Chemical Design Using a Data-Driven Continuous Representation of Molecules’, *ACS Cent. Sci.*, vol. 4, no. 2, pp. 268–276, 2018, doi: 10.1021/acscentsci.7b00572.
- [42] D. Polykovskiy *et al.*, ‘Molecular Sets (MOSES): A Benchmarking Platform for Molecular Generation Models’, *Front. Pharmacol.*, vol. 11, pp. 1–19, Nov. 2020, doi: 10.3389/fphar.2020.565644.
- [43] N. Brown, M. Fiscato, M. H. S. Segler, and A. C. Vaucher, ‘GuacaMol: Benchmarking Models for de Novo Molecular Design’, *J. Chem. Inf. Model.*, vol. 59, no. 3, pp. 1096–1108, 2019, doi: 10.1021/acs.jcim.8b00839.
- [44] I. Goodfellow *et al.*, ‘Generative adversarial networks’, *Commun. ACM*, vol. 63, no. 11, pp. 139–144, 2020, doi: 10.1145/3422622.
- [45] L. Yang *et al.*, ‘Diffusion Models: A Comprehensive Survey of Methods and Applications’, *ACM Comput. Surv.*, vol. 56, no. 4, 2023, doi: 10.1145/3626235.
- [46] J. B. Tenenbaum, V. De Silva, and J. C. Langford, ‘A global geometric framework for nonlinear dimensionality reduction’, *Science (80-.)*, vol. 290, no. 5500, pp. 2319–2323, Dec. 2000, doi: 10.1126/science.290.5500.2319.
- [47] D. Flam-Shepherd, K. Zhu, and A. Aspuru-Guzik, ‘Language models can learn complex molecular distributions’, *Nat. Commun.*, vol. 13, no. 1, pp. 1–10, Jun. 2022, doi: 10.1038/s41467-022-30839-x.
- [48] Y. Chen *et al.*, ‘Molecular language models: RNNs or transformer?’, *Brief. Funct. Genomics*, vol. 22, no. 4, pp. 392–400, 2023, doi: 10.1093/bfpg/eland012.
- [49] M. Eppe, C. Gumbsch, M. Kerzel, P. D. H. Nguyen, M. V. Butz, and S. Wermter, ‘Intelligent problem-solving as integrated hierarchical reinforcement learning’, *Nat. Mach. Intell.*, vol. 4, no. 1, pp. 11–20, 2022, doi: 10.1038/s42256-021-00433-9.
- [50] Y. Bengio, A. Courville, and P. Vincent, ‘Representation learning: A review and new perspectives’, *IEEE Trans. Pattern Anal. Mach. Intell.*, vol. 35, no. 8, pp. 1798–1828, 2013, doi: 10.1109/TPAMI.2013.50.
- [51] J. Loula, M. Baroni, and B. M. Lake, ‘Rearranging the Familiar: Testing Compositional Generalization in Recurrent Networks’, *EMNLP 2018 - 2018 EMNLP Work. BlackboxNLP Anal. Interpret. Neural Networks NLP, Proc. 1st Work.*, pp. 108–114, 2018, doi: 10.18653/v1/w18-5413.
- [52] B. M. Lake, T. D. Ullman, J. B. Tenenbaum, and S. J. Gershman, ‘Building machines that learn and think like people’, *Behav. Brain Sci.*, vol. 40, 2017, doi: 10.1017/S0140525X16001837.
- [53] R. MONTAGUE, ‘Universal grammar’, *Theoria*, vol. 36, no. 3, pp. 373–398, 1970, doi: 10.1111/j.1755-

- 2567.1970.tb00434.x.
- [54] R. B. Lees and N. Chomsky, 'Syntactic Structures', *Language*, vol. 33, no. 3. JSTOR, p. 375, 1957. doi: 10.2307/411160.
 - [55] D. Hupkes, V. Dankers, M. Mul, and E. Bruni, 'Compositionality Decomposed: How do Neural Networks Generalise?', *J. Artif. Intell. Res.*, vol. 67, pp. 757–795, 2020, doi: 10.1613/JAIR.1.11674.
 - [56] B. Lake and M. Baroni, 'Generalization without systematicity: On the compositional skills of sequence-to-sequence recurrent networks', *35th Int. Conf. Mach. Learn. ICML 2018*, vol. 7, pp. 4487–4499, 2018.
 - [57] G. Lample and F. Charton, 'Deep Learning for Symbolic Mathematics', *8th Int. Conf. Learn. Represent. ICLR 2020*, pp. 1–24, 2020.
 - [58] A. Wang, A. Singh, J. Michael, F. Hill, O. Levy, and S. R. Bowman, 'GLUE: A Multi-Task Benchmark and Analysis Platform for Natural Language Understanding', *EMNLP 2018 - 2018 EMNLP Work. BlackboxNLP Anal. Interpret. Neural Networks NLP, Proc. 1st Work.*, pp. 353–355, 2018, doi: 10.18653/v1/w18-5446.
 - [59] J. Wei *et al.*, 'Emergent Abilities of Large Language Models', *Trans. Mach. Learn. Res.*, 2022, [Online]. Available: <http://arxiv.org/abs/2206.07682>
 - [60] D. Hendrycks, X. Liu, E. Wallace, A. Dziedziec, R. Krishnan, and D. Song, 'Pretrained transformers improve out-of-distribution robustness', *Proc. Annu. Meet. Assoc. Comput. Linguist.*, pp. 2744–2751, 2020, doi: 10.18653/v1/2020.acl-main.244.
 - [61] T. Bai *et al.*, 'A Survey of Multimodal Large Language Model from A Data-centric Perspective', pp. 1–40, 2024, [Online]. Available: <http://arxiv.org/abs/2405.16640>
 - [62] J. Kaplan *et al.*, 'Scaling Laws for Neural Language Models', *arXiv*, 2020, [Online]. Available: <http://arxiv.org/abs/2001.08361>
 - [63] J. Hoffmann *et al.*, 'Training Compute-Optimal Large Language Models', *Adv. Neural Inf. Process. Syst.*, vol. 35, no. 2020, pp. 1–36, 2022.
 - [64] D. Yogatama *et al.*, 'Learning and Evaluating General Linguistic Intelligence', *arXiv*, Jan. 2019, Accessed: Aug. 31, 2024. [Online]. Available: <http://arxiv.org/abs/1901.11373>
 - [65] R. Thomas McCoy, E. Pavlick, and T. Linzen, 'Right for the wrong reasons: Diagnosing syntactic heuristics in natural language inference', *ACL 2019 - 57th Annu. Meet. Assoc. Comput. Linguist. Proc. Conf.*, no. 2, pp. 3428–3448, 2020, doi: 10.18653/v1/p19-1334.
 - [66] S. Gururangan, S. Swayamdipta, O. Levy, R. Schwartz, S. R. Bowman, and N. A. Smith, 'Annotation artifacts in natural language inference data', *NAACL HLT 2018 - 2018 Conf. North Am. Chapter Assoc. Comput. Linguist. Hum. Lang. Technol. - Proc. Conf.*, vol. 2, pp. 107–112, Mar. 2018, doi: 10.18653/v1/n18-2017.
 - [67] T. Niven and H. Y. Kao, 'Probing Neural Network Comprehension of Natural Language Arguments', *ACL 2019 - 57th Annu. Meet. Assoc. Comput. Linguist. Proc. Conf.*, pp. 4658–4664, Jul. 2019, doi: 10.18653/v1/p19-1459.
 - [68] T. B. Brown *et al.*, 'Language models are few-shot learners', *Adv. Neural Inf. Process. Syst.*, vol. 2020-Decem, 2020.
 - [69] K. M. Jablonka, P. Schwaller, A. Ortega-Guerrero, and B. Smit, 'Leveraging large language models for predictive chemistry', *Nat. Mach. Intell.*, vol. 6, no. 2, pp. 161–169, 2024, doi: 10.1038/s42256-023-00788-1.
 - [70] X. Mai *et al.*, 'From Efficient Multimodal Models to World Models: A Survey', *arXiv*, pp. 1–19, 2024, [Online]. Available: <http://arxiv.org/abs/2407.00118>
 - [71] T. Bai *et al.*, 'A Survey of Multimodal Large Language Model from A Data-centric Perspective_EC', 2024, [Online]. Available: <http://arxiv.org/abs/2405.16640>
 - [72] G. F. Marcus *et al.*, 'Rethinking Eliminative Connectionism', *Cogn. Psychol.*, vol. 282, no. 37, pp. 243–282, 1998.
 - [73] A. K. Nigam *et al.*, 'TARTARUS: A Benchmarking Platform for Realistic And Practical Inverse Molecular Design', *Adv. Neural Inf. Process. Syst.*, vol. 36, Sep. 2023, Accessed: Feb. 28, 2024. [Online]. Available: <https://arxiv.org/abs/2209.12487v4>
 - [74] Z. Zhang, F. Li, J. Guan, Z. Kong, L. Shi, and S. Zhou, 'GANs for Molecule Generation in Drug Design and Discovery', *Intell. Syst. Ref. Libr.*, 2022, doi: 10.1007/978-3-030-91390-8_11.
 - [75] D. J. Rezende and S. Mohamed, 'Variational inference with normalizing flows', *32nd Int. Conf. Mach. Learn. ICML 2015*, vol. 2, pp. 1530–1538, 2015.
 - [76] M. Beck *et al.*, 'xLSTM: Extended Long Short-Term Memory', pp. 1–55, 2024, [Online]. Available: <http://arxiv.org/abs/2405.04517>
 - [77] R. Özçelik, S. de Ruiter, E. Criscuolo, and F. Grisoni, 'Chemical language modeling with structured state space sequence models', *Nat. Commun.*, vol. 15, no. 1, pp. 1–12, Jul. 2024, doi: 10.1038/s41467-024-50469-9.
 - [78] K. Guo, 'What can Large Language Models do in chemistry? A comprehensive benchmark on eight tasks_EC', no. NeurIPS, 2023.
 - [79] M. A. Skinnider, 'Invalid SMILES are beneficial rather than detrimental to chemical language models', *Nat. Mach. Intell.*, pp. 1–12, Mar. 2024, doi: 10.1038/s42256-024-00821-x.
 - [80] Z. Ji *et al.*, 'Survey of Hallucination in Natural Language Generation', *ACM Comput. Surv.*, vol. 1, Accessed: Sep. 14, 2024. [Online]. Available: <https://doi.org/>
 - [81] A. Gaulton *et al.*, 'ChEMBL: A large-scale bioactivity database for drug discovery', *Nucleic Acids Res.*, vol. 40, no. D1, Jan. 2012, doi: 10.1093/NAR/GKR777.
 - [82] T. Sterling and J. J. Irwin, 'ZINC 15 - Ligand Discovery for Everyone', *J. Chem. Inf. Model.*, vol. 55, no. 11, pp. 2324–2337, Nov. 2015, doi: 10.1021/acs.jcim.5b00559.
 - [83] L. C. Blum and J. L. Reymond, '970 Million druglike small molecules for virtual screening in the chemical universe

- database GDB-13', *J. Am. Chem. Soc.*, vol. 131, no. 25, pp. 8732–8733, Jul. 2009, doi: 10.1021/JA902302H/SUPPL_FILE/JA902302H_SI_001.PDF.
- [84] J. J. Irwin and B. K. Shoichet, 'ZINC-A Free Database of Commercially Available Compounds for Virtual Screening', 2005, doi: 10.1021/C1049714.
 - [85] J. Hachmann *et al.*, 'The harvard clean energy project: Large-scale computational screening and design of organic photovoltaics on the world community grid', *J. Phys. Chem. Lett.*, vol. 2, no. 17, pp. 2241–2251, Sep. 2011, doi: 10.1021/JZ200866S/ASSET/IMAGES/LARGE/JZ-2011-00866S_0005.JPEG.
 - [86] P. C. St John *et al.*, 'Message-passing neural networks for high-throughput polymer screening', *J. Chem. Phys.*, vol. 150, no. 23, p. 234111, Jun. 2019, doi: 10.1063/1.5099132.
 - [87] S. Kullback and R. A. Leibler, 'On Information and Sufficiency', *Ann. Math. Stat.*, vol. 22, pp. 79–86, 1951, doi: 10.1214/AOMS/1177729694.
 - [88] K. Preuer, P. Renz, T. Unterthiner, S. Hochreiter, and G. Klambauer, 'Fréchet ChemNet Distance: A Metric for Generative Models for Molecules in Drug Discovery', *J. Chem. Inf. Model.*, vol. 58, no. 9, pp. 1736–1741, Sep. 2018, doi: 10.1021/acs.jcim.8b00234.
 - [89] P. Ertl and A. Schuffenhauer, 'Estimation of synthetic accessibility score of drug-like molecules based on molecular complexity and fragment contributions', *J. Cheminform.*, vol. 1, no. 1, 2009, doi: 10.1186/1758-2946-1-8.